# "Constrained Geometry" Group 3 Metal Complexes of the Fluorenyl-Based Ligands [(3,6-$^t$Bu$_2$Flu)SiR$_2$N$^t$Bu]: Synthesis, Structural Characterization, and Polymerization Activity

Evgueni Kirillov,[†] Loic Toupet,[‡] Christian W. Lehmann,[§] Abbas Razavi,[∥] and Jean-François Carpentier*,[†]

*Organométalliques et Catalyse, UMR 6509 CNRS, and Groupe Matière Condensée et Matériaux, Cristallochimie, UMR 6626 CNRS, Université de Rennes 1, 35042 Rennes Cedex, France, Max-Planck-Institut für Kohlenforschung, Chemical Crystallography, Postfach 101353, 45466 Mülheim/Ruhr, Germany, and Atofina Research, Zone Industrielle C, 7181 Feluy, Belgium*

*Received June 3, 2003*

Downloaded by CARLI CONSORTIUM on June 29, 2009
Published on September 30, 2003 on http://pubs.acs.org | doi: 10.1021/om0304210

Alkane elimination between Y(CH$_2$SiMe$_3$)$_3$(THF)$_2$ and the diprotio ligands [(3,6-$^t$Bu$_2$C$_{13}$H$_7$)SiR$_2$NH$^t$Bu] (R = Me, **1a**; R = Ph, **1b**) gave [$\eta^3$:$\eta^1$-((3,6-$^t$Bu$_2$C$_{13}$H$_6$)SiR$_2$N$^t$Bu)Y(CH$_2$SiMe$_3$)(THF)$_2$] (R = Me, **2a**; R = Ph, **2b**). **2a** is thermally stable in toluene solution and shows a dynamic behavior connected to THF dissociation, while **2b** is thermally unstable. Reaction of **2a** with H$_2$ or PhSiH$_3$ led to the putative hydrido complex "[(3,6-$^t$Bu$_2$Flu)SiMe$_2$N$^t$Bu)YH(THF)]$_n$" (**3**). Deprotonation of **1a** with 1 and 2 equiv of $^n$BuLi gave [(3,6-$^t$Bu$_2$C$_{13}$H$_6$)SiMe$_2$NH$^t$Bu]Li (**5**) and [(3,6-$^t$Bu$_2$C$_{13}$H$_6$)SiMe$_2$N$^t$Bu]Li$_2$ (**4**), respectively, both of which were characterized crystallographically. Salt elimination reactions between LnCl$_3$(THF)$_n$ precursors (Ln = Y, La, Nd) and 1 equiv of **4** gave mixtures of complexes, from which ionic complexes that contain two chelated ligands per lanthanide center, [{$\eta^3$:$\eta^1$-(3,6-$^t$Bu$_2$C$_{13}$H$_6$)SiMe$_2$N$^t$Bu}$_2$Ln]$^-$[Li(solvent)$_n$]$^+$ (Ln = Y, solvent = THF, $n$ = 4, **6**; Ln = La, solvent = THF, $n$ = 4, **7**; Ln = La, solvent = Et$_2$O, $n$ = 2, **8**; Ln = Nd, solvent = THF, $n$ = 4, **9**), were isolated. The neutral dimeric chloro complex [$\eta^5$:$\eta^1$-((3,6-$^t$Bu$_2$C$_{13}$H$_6$)SiMe$_2$N$^t$Bu)Nd($\mu$-Cl)(THF)]$_2$ (**10**) was also crystallized from the crude metathesis product. The solid-state structures of **2a**, **8**, **9**, and **10** show versatile coordination modes of the fluorenyl ligands, either $\eta^3$ or $\eta^5$ symmetric, involving carbon atoms of the central Cp ring (**8** and **10**), or unusual $\eta^3$ dissymmetric, involving carbon atoms of the central Cp and one adjacent phenyl rings (**2a** and **9**). Some of the complexes obtained were explored as catalysts for ethylene and MMA polymerization.

## Introduction

Half-sandwich complexes of group 3 metals[1] that contain linked cyclopentadienyl−amido ligands have attracted considerable attention. First designed by Bercaw for organoscandium olefin polymerization "constrained geometry catalysts" (CGC),[2] these ligands have been extensively applied in and developed for group 4 metal chemistry.[3] Recent years have witnessed a renewal with group 3 metals.[1h] Thus, the groups of Piers,[4] Okuda,[5] Marks,[6] and Hou[7] have reported a variety of rare-earth complexes of bifunctional ligands having the formula [Ln($\eta^5$:$\eta^1$-C$_5$Me$_4$SiMe$_2$NR)X(L)$_n$]$_m$ (Ln = Sc, Y, Sm, Nd, Lu, Yb; R = $^t$Bu, aryl; X = H, carbyl, NR$_2$; L =

* To whom correspondence should be addressed. Fax: (+33)(0)223-236-939. E-mail: jean-francois.carpentier@univ-rennes1.fr.
[†] Organométalliques et Catalyse, Université de Rennes 1.
[‡] Groupe Matière Condensée et Matériaux, Université de Rennes 1.
[§] Max-Planck-Institut für Kohlenforschung.
[∥] Atofina Research.

(1) Recent organolanthanide reviews: (a) Schumann, H.; Meese-Marktscheffel, J. A.; Esser, L. *Chem. Rev.* **1995**, *95*, 865. (b) Anwander, R.; Herrmann, W. A. *Top. Curr. Chem.* **1996**, *179*, 1. (c) Edelmann, F. T. *Top. Curr. Chem.* **1996**, *179*, 247. (d) Anwander, R. In *Applied Homogeneous Catalysis with Organometallic Compounds*; Cornils, B., Herrmann, W. A., Eds.; Wiley: Weinheim, Germany, 1996; Vol. 2, p 866. (e) Molander, G. A. *Chemtracts: Org. Chem.* **1998**, *11*, 237. (f) Anwander, R. *Top. Organomet. Chem.* **1999**, *2*, 1. (g) Molander, G. A.; Dowdy, E. C. *Top. Organomet. Chem.* **1999**, *2*, 119. (h) For a comprehensive review on mono(cyclopentadienyl) complexes, see: Arndt, S.; Okuda, J. *Chem. Rev.* **2002**, *102*, 1953. (i) Hou, Z.; Wakatsuki, Y. *Coord. Chem. Rev.* **2002**, *231*, 1.

(2) (a) Shapiro, P. J.; Bunel, E.; Schaefer, W. P.; Bercaw, J. E. *Organometallics* **1990**, *9*, 867. (b) Piers, W. E.; Shapiro, P. J.; Bunel, E. E.; Bercaw, J. E. *Synlett* **1990**, 74. (c) Shapiro, P. J.; Cotter, W. D.; Schaefer, W. P.; Labinger, J. A.; Bercaw, J. E. *J. Am. Chem. Soc.* **1994**, *116*, 4623.

(3) For reviews, see: (a) McKnight, A. L.; Waymouth, R. M. *Chem. Rev.* **1998**, *98*, 2587. (b) Gibson, V. C.; Spitzmesser, S. K. *Chem. Rev.* **2003**, *103*, 283.

(4) Mu, Y.; Piers, W. E.; MacDonald, M.-A.; Zaworotko, M. J. *Can. J. Chem.* **1995**, *73*, 2233.

(5) (a) Hultzsch, K. C.; Spaniol, T. P.; Okuda, J. *Angew. Chem., Int. Ed.* **1999**, *38*, 227. (b) Hultzsch, K. C.; Voth, P.; Beckerle, K.; Spaniol, T. P.; Okuda, J. *Organometallics* **2000**, *19*, 228. (c) Arndt, S.; Voth, P.; Spaniol, T. P.; Okuda, J. *Organometallics* **2000**, *19*, 4690. (d) Okuda, J.; Arndt, S.; Beckerle, K.; Hultzsch, K. C.; Voth, P.; Spaniol, T. P. *Pure Appl. Chem.* **2001**, *73*, 351. (e) Okuda, J.; Arndt, S.; Beckerle, K.; Hultzsch, K. C.; Voth, P.; Spaniol, T. P. In *Organometallic Catalysts and Olefin Polymerization*; Blom, R., Follestad, A., Rytter, E., Tilset, M., Ystenes, M., Eds.; Springer: Berlin, 2001; p 156. (f) Arndt, S.; Trifonov, A.; Spaniol, T. P.; Okuda, J.; Kitamura, M.; Takahashi, T. *J. Organomet. Chem.* **2002**, *647*, 158. (g) Voth, P.; Arndt, S.; Spaniol, T. P.; Okuda, J.; Ackerman, L. J.; Green, M. L. H. *Organometallics* **2003**, *22*, 65.

10.1021/om0304210 CCC: $25.00 © 2003 American Chemical Society
Publication on Web 09/30/2003

Downloaded by CARLI CONSORTIUM on June 29, 2009
Published on September 30, 2003 on http://pubs.acs.org | doi: 10.1021/om0304210

THF, $PMe_3$; $n = 0-3$; $m = 1, 2$) and explored their reactivity in some catalytic processes. Studies were also concerned with "less constrained geometry" complexes of the type $[Y(\eta^5:\eta^1\text{-}C_5Me_4CH_2SiMe_2N^tBu)(CH_2SiMe_3)(THF)]$,[8] complexes of the tridentate ligands $(C_5Me_4H)SiMe_2NHCH_2CH_2R$ (R = OMe, $NMe_2$),[9,10] and recently divalent lanthanide complexes such as $Ln(\eta^5:\eta^1\text{-}C_5Me_4SiMe_2NPh)X(THF)_n$ (Ln = Sm, Yb; $n = 0-3$)[11] and $Li[Yb\{\eta^5:\eta^1\text{-}(3\text{-}^tBuC_5H_3)SiMe_2NCH_2CH_2X\}_2]$ (X = $NMe_2$, OMe).[12]

As it appears from the aforementioned examples, almost all of the constrained-geometry group 3 metal complexes prepared so far are based on silylene-bridged *cyclopentadienyl*−amido ligands.[13] To our knowledge, $[Y(\eta^5:\eta^1\text{-}C_9H_6SiMe_2N^tBu)(CH_2SiMe_3)(THF)]$ constitutes the sole congener of these half-sandwich lanthanide complexes that bears a linked *indenyl*−amido ligand,[5b] and there is so far no example of a constrained-geometry organolanthanide complex based on a *fluorenyl* ligand.[14] This situation, which contrasts markedly with the variety of indenyl− and fluorenyl−amido ligands that have been successfully associated to group 4 metals,[3] largely stems from the synthetic difficulties encountered in the preparation of constrained-geometry organolanthanides. The latter remain essentially limited to alkane[5a,6,9] and amine[4,11a] eliminations, which have a quite limited scope due to the thermal sensitivity of lanthanide carbyl precursors[6a] and the moderate basicity of lanthanide amido precursors, respectively. On the other hand, the traditional salt elimination approach is often plagued by the formation of undesired products, such as ate complexes.[1] We report here a new series of silylene-bridged *fluorenyl*−amido organolanthanide complexes derived from the ligands $[(3,6\text{-}^tBu_2\text{-}C_{13}H_7)SiR_2NH^tBu]$ (R = Me, Ph). These ligands have been selected for this study because (i) the two *tert*-butyl groups on fluorene at the 3,6-positions should simplify $^1H$ NMR patterns, (ii) we expect an increase in solubility of complexes as compared to nonsubstituted fluorene−amido ligands, and (iii) they have played a unique role in group 4 metal chemistry.[15] The coordination of these ligands onto lanthanides (Y, La, Nd) was investigated using amine and alkane elimination routes as well as salt elimination reactions.

## Results and Discussion

**Amine and Alkane Elimination Reactions.** Amine[4,11a] and alkane[5a,6,9] elimination reactions were investigated as privileged routes, since both of these previously proved efficient for the preparation of *cyclopentadienyl*−amido as well as *indenyl*−amido neutral organolanthanide complexes. First, we observed that the lanthanide amides $Ln[N(SiMe_3)_2]_3$ (Ln = Y, La) and $Y[N(SiHMe_2)_2]_3(THF)_2$ do not react with the diprotio ligands $(3,6\text{-}^tBu_2C_{13}H_7)SiR_2NH^tBu$ (R = Me, **1a**; R = Ph, **1b**), either in THF-$d_8$ or in toluene-$d_8$, even on heating above the boiling points of the solvents. In both cases, the reagents were found intact after 1 week under these conditions (eq 1).[16] Earlier studies from our group have

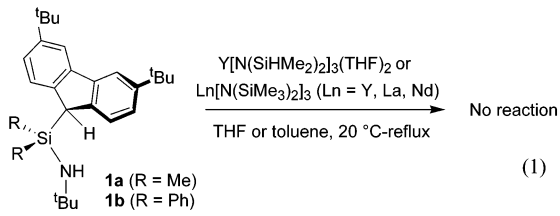

(1)

shown that amine elimination between $Ln[N(SiMe_3)_2]_3$ (Ln = Y, La, Nd) and Cp*H*$CMe_2$Flu*H* in THF proceeds via the rapidly formed intermediates $(\eta^5\text{-}CpCMe_2FluH)Ln[N(SiMe_3)_2]_2$, which undergo readily ligand redistribution reactions (5−20 °C, minutes) to give the mono(amido)lanthanide complexes $(\eta^5\text{-}CpCMe_2FluH)_2Ln[N(SiMe_3)_2]$; then, subsequent intramolecular amine elimination between the remaining amido group and a pending fluorenyl moiety takes place under THF reflux to yield the *ansa* complexes $(\eta^5:\eta^5\text{-}CpCMe_2Flu)Ln(\eta^5\text{-}CpCMe_2FluH)$.[14g] These results suggest that the inertness of **1a**,**b** toward lanthanide amides does not stem

(6) (a) Tian, S.; Arredondo, V. M.; Stern, C. L.; Marks, T. J. *Organometallics* **1999**, *18*, 2568. (b) Arredondo, V. M.; Tian, S.; McDonald, F. E.; Marks, T. J. *J. Am. Chem. Soc.* **1999**, *121*, 3633. (c) Douglass, M. R.; Stern, C. L.; Marks, T. J. *J. Am. Chem. Soc.* **2001**, *123*, 10221. (d) Ryu, J.-S.; Marks, T. J.; McDonald, F. E. *Org. Lett.* **2001**, *3*, 3091. (e) Hong, S.; Marks, T. J. *J. Am. Chem. Soc.* **2002**, *124*, 7886.

(7) Nishiura, M.; Hou, Z.; Wakatsuki, Y.; Yamaki, T.; Miyamoto, T. *J. Am. Chem. Soc.* **2003**, *125*, 1184.

(8) Trifonov, A. A.; Spaniol, T. P.; Okuda, J. *Organometallics* **2001**, *20*, 4869.

(9) Mu, Y.; Piers, W. E.; MacQuarrie, D. C.; Zaworotko, M. J.; Young, V. G. *Organometallics* **1996**, *15*, 2720.

(10) (a) Hultzsch, K. C.; Spaniol, T. P.; Okuda, J. *Organometallics* **1997**, *16*, 4845. (b) Yoder, J. C.; Day, M. W.; Bercaw, J. E. *Organometallics* **1998**, *17*, 4946.

(11) (a) Hou, Z.; Koizumi, T.; Nishiura, M.; Wakatsuki, Y. *Organometallics* **2001**, *20*, 3323. (b) Hou, Z.; Wakatsuki, Y. *J. Organomet. Chem.* **2002**, *647*, 61.

(12) Trifonov, A. T.; Spaniol, T. P.; Okuda, J. *Eur. J. Inorg. Chem.* **2003**, 926.

(13) For constrained-geometry organolanthanide complexes based on silylene-linked cyclopentadienyl−non-amido ligands: (a) Tardif, O.; Hou, Z.; Nishiura, M.; Koizumi, T.; Wakatsuki, Y. *Organometallics* **2001**, *20*, 4565. (b) Arndt, S.; Spaniol, T. P.; Okuda, J. *Organometallics* **2003**, *22*, 775.

(14) For *ansa*-organolanthanidocene complexes that contain a bridged *fluorenyl* ligand, see the following. (a) $(\eta^5:\eta^5\text{-}FluSiMe_2Cp')Y[N(SiMe_3)_2]$: Lee, M. H.; Hwang, J.-W.; Kim, Y.; Kim, J.; Han, Y.; Do, Y. *Organometallics* **1999**, *18*, 5124. (b) $[(\eta^5:\eta^5\text{-}FluSiR_2Cp')Ln(\mu\text{-}Cl)]_2$ (R = Me, Ph; Ln = Y, Lu, Dy, Er) and $(\eta^5:\eta^5\text{-}FluSiMe_2Cp)Ln[E(SiMe_3)_2]$ (Ln = Dy, Er, E = N, CH): Qian, C.; Nie, W.; Sun, J. *Organometallics* **2000**, *19*, 4134. (c) $[(\eta^5:\eta^5\text{-}FluCPh_2Cp)LnCl_2][Li(THF)_4]$ (Ln = Lu, Y): Qian, C.; Nie, W.; Sun, J. *J. Chem. Soc., Dalton Trans.* **1999**, 3283. (d) $[(\eta^5:\eta^5\text{-}FluCPh_2Cp)Nd(BH_4)_2][K(18\text{-crown-}6)]$: Qian, C.; Nie, W.; Sun, J. *J. Organomet. Chem.* **2001**, *626*, 171. (e) $(\eta^5:\eta^5\text{-}FluCPh_2Cp)Lu(N(SiMe_3)_2)$: Qian, C.; Nie, W.; Sun, J. *J. Organomet. Chem.* **2002**, *645*, 82; See also: (f) Nie, W.; Qian, C.; Chen, Y.; Sun, J. *J. Organomet. Chem.* **2002**, *647*, 114. (g) $(\eta^5:\eta^5\text{-}CpCMe_2Flu)Ln(\eta^5\text{-}CpCMe_2FluH)(THF)_n$ (Ln = Y, La, Nd; $n = 0, 1$): Dash, A., K.; Razavi, A.; Mortreux, A.; Lehmann, C.; Carpentier, J.-F. *Organometallics* **2002**, *21*, 3238.

(15) (a) Razavi, A. Thewalt, U. *J. Organomet. Chem.* **2001**, *621*, 267. (b) Razavi, A.; Baekelmans, D.; Bellia, V.; De Brauwer, Y.; Hortmann, K.; Lambrecht, M.; Miserque, O.; Peters, L.; Slawinski, M.; Van Belle, S. In *Organometallic Catalysts for Olefin Polymerization*, Blom, R., Ed.; Springer-Verlag: Berlin, 2001; pp 267−279. For other group 4 metal constrained-geometry complexes having nonsubstituted fluorenyl−amido ligands, see: (c) Hasan, T.; Nishii, K.; Shiono, T.; Ikeda, T. *Macromolecules* **2002**, *35*, 8933 and references therein. (d) Xu, G.; Cheng, D. *Macromolecules* **2001**, *34*, 2040 and references therein.

(16) A possible explanation for this nonreactivity is the lower acidity of the fluorenyl proton in **1a**,**b**, as compared to that of the cyclopentadienyl and indenyl equivalents. Standard p$K_a$ values: Cp*H*, 16; Ind*H*, 20; Flu*H*, 23. See the following: (a) March, J. *Advanced Organic Chemistry*, 4th ed.; Wiley: New York, 1992; Chapter 8. (b) Bordwell, F. G.; Bausch, M. J. *J. Am. Chem. Soc.* **1983**, *105*, 6188. (c) p$K_a$ values in $C_6D_6$/THF-$d_8$ (20:1) determined according to the modified method of Fraser: Flu*H*, 24.0−24.2; Ind*H*, 21.7; 9-$(SiHMe_2)$-Flu*H*, 23.1; 3-$(SiHMe_2)$-Ind*H*, 20.2; 2-Me-Ind*H*, 23.1. Eppinger, J.; Spiegler, M.; Hieringer, W.; Herrmann, W. A.; Anwander, R. *J. Am. Chem. Soc.* **2000**, *122*, 3080. An alternative, more complicated mechanism for the initial metalation involving $\pi$-donation of the cyclopentadienyl group to the lanthanide has been proposed to account for the fairly good reactivity of relatively low acidic derivatives, e.g. $Me_2Si(C_5Me_4H)$.[16c]

**Table 1. Summary of Crystallographic Data**

| | **2a** | **4**·0.5(toluene) | **5** | **8** | **9**·(toluene)·THF | **10** |
|---|---|---|---|---|---|---|
| formula | $C_{39}H_{66}NO_2Si_2Y$ | $C_{42.50}H_{67}NO_3SiLi_2$ | $C_{31}H_{50}NO_2SiLi$ | $C_{62}H_{98}N_2O_2Si_2LiLa$ | $C_{85}H_{134}LiN_2NdO_6Si_2$ | $C_{62}H_{94}Cl_2N_2Nd_2O_2Si_2$ |
| cryst size, mm | 0.10 × 0.09 × 0.05 | 0.19 × 0.15 × 0.11 | 0.48× 0.33 × 0.33 | 0.46 × 0.36 × 0.34 | 0.42 × 0.38 × 0.32 | 0.36 × 0.32 × 0.32 |
| mol wt | 716.95 | 681.94 | 503.75 | 1105.46 | 1487.30 | 1314.95 |
| cryst syst | monoclinic | monoclinic | monoclinic | monoclinic | monoclinic | monoclinic |
| space group | $P2_1/n$ | $P2_1/c$ | $P2_1/n$ | $Cc$ | $P2_1/c$ | $A2/a$ |
| $a$, Å | 12.3702(5) | 24.1847(3) | 11.7950(4) | 24.4430(2) | 13.6015(2) | 11.0801(1) |
| $b$, Å | 23.0023(11) | 16.5846(2) | 19.2352(2) | 14.2723(2) | 20.0120(2) | 26.0401(3) |
| $c$, Å | 14.9881(7) | 22.2003(3) | 14.9331(6) | 19.9580(2) | 30.4072(4) | 23.2813(3) |
| α, deg | 90 | 90 | 90 | 90 | 90 | 90 |
| $\beta$, deg | 106.021(2) | 113.0210(10) | 108.653(1) | 118.955(1) | 97.426(1) | 97.869(1) |
| $\gamma$, deg | 90 | 90 | 90 | 90 | 90 | 90 |
| $V$, Å$^3$ | 4099.1(3) | 8195.26(18) | 3210.0(2) | 6092.2(1) | 8207.2(2) | 6654.0(1) |
| $Z$ | 4 | 8 | 4 | 4 | 4 | 4 |
| $D_{calcd}$, g cm$^{-3}$ | 1.162 | 1.105 | 1.042 | 1.205 | 1.202 | 1.313 |
| $T$, K | 100(2) | 100(2) | 110(1) | 110(2) | 120(2) | 120(2) |
| $\theta$ range, deg | 5.30−23.38 | 4.55−26.40 | 1.79−27.53 | 1.72−27.49 | 2.53−27.48 | 2.09−27.49 |
| $\mu$, mm$^{-1}$ | 1.511 | 0.094 | 0.098 | 0.781 | 0.711 | 1.698 |
| no. of measd rflns | 22 815 | 89 182 | 31 822 | 61 586 | 87 138 | 15 613 |
| no. of indep rflns | 5842 | 16 703 | 7386 | 6916 | 18 574 | 7629 |
| no. of rflns with $I > 2\sigma(I)$ | 3431 | 10 741 | 4056 | 6634 | 12 224 | 5331 |
| no. of params | 417 | 915 | 329 | 649 | 849 | 326 |
| goodness of fit | 1.048 | 1.058 | 1.030 | 1.059 | 1.048 | 1.017 |
| R1 ($I > 2\sigma(I)$) | 0.0766 | 0.0787 | 0.0682 | 0.0304 | 0.064 | 0.037 |
| wR2 | 0.1558 | 0.1556 | 0.1632 | 0.0753 | 0.144 | 0.084 |
| largest diff, e Å$^{-3}$ | 0.632/−0.482 | 0.520/−0.291 | 0.405/−0.451 | 2.47/−0.715 | 2.650/−0.996 | 1.241/−0.618 |

Downloaded by CARLI CONSORTIUM on June 29, 2009
Published on September 30, 2003 on http://pubs.acs.org | doi: 10.1021/om0304210

only from the poor acidity of the fluorenyl functionality.[16] Indeed, because of the ability of $SiR_3$ groups to stabilize negative charges at the α-position, the fluorenyl proton in **1a**,**b** is much more acidic than that in $CpHCMe_2FluH$.[16c] Rather, they suggest that preliminary coordination of the other functionality of the ansa ligand, i.e., Cp−H for the carbon-bridged ligand and $^t$BuN−H for **1a**,**b**, which in turn enforces the pending fluorenyl moiety in the coordination sphere or immediate proximity of the metal center, may be a prerequisite for the proton transfer from the fluorenyl fragment to the amido moiety to occur. This initial process easily takes place with $CpHCMe_2FluH$ (vide supra) but does not for **1a**,**b**, likely because the $^t$BuN−H functionality is even less acidic than the fluorenyl group (vide infra).[16,17]

In contrast to amine elimination, alkane elimination is a more efficient synthetic route, likely because Ln−C bonds are protonically more reactive.[1] In situ monitoring by $^1$H NMR spectroscopy showed that $Y(CH_2SiMe_3)_3(THF)_2$ reacts with 1 equiv of diprotio ligand **1a** at room temperature in benzene to give $[(3,6\text{-}^t Bu_2C_{13}H_6)SiMe_2N^tBu]Y(CH_2SiMe_3)(THF)_2$ (**2a**), with concomitant release of 2 equiv of $SiMe_4$ (eq 2). No intermediate could

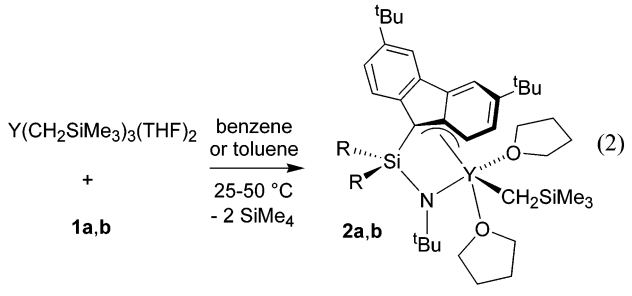

(2)

be detected, suggesting that coordination of the second functionality ($^t$BuN−H or Flu−H) proceeds faster than the first one (Flu−H or $^t$BuN−H). The conversion of **1a** was 37% after 1 h at 20 °C, with >98% selectivity for **2a**, and reached a plateau at 90% after a few days, where no more starting carbyl complex was detected. Quantitative conversion of **1a** to **2a** was achieved by adding 0.3 extra equiv (vs **1a**) of $Y(CH_2SiMe_3)_3(THF)_2$ to the reaction mixture. Increase of the temperature to 50 °C slightly accelerated the reaction of **1a** and $Y(CH_2SiMe_3)_3(THF)_2$, but it proved again necessary to re-add some carbyl precursor after a while to achieve total conversion of the ligand. Adjustment of the reaction balance is likely due to slow decomposition of $Y(CH_2SiMe_3)_3(THF)_2$, which is quite thermally sensitive.[18] Complex **2a** is stable in benzene solution at 50 °C for several hours without noticeable decomposition, in contrast to the parent yttrium complex $(C_5Me_4SiMe_2N^tBu)Y(CH_2SiMe_3)(THF)$ (half-life 600 ± 10 min at 50 °C in $C_6D_6$).[5b] The synthesis of **2a** was conveniently carried out on a gram scale batch by generation of in situ $Y(CH_2SiMe_3)_3(THF)_2$ from $YCl_3(THF)_{3.5}$ and $LiCH_2SiMe_3$, subsequent protonolysis with **1a**, and crystallization from pentane at −35 °C to give yellow crystals in 68% yield. The new carbyl complex **2a** was characterized by elemental analysis, NMR, and an X-ray diffraction study (Table 1).

In the solid state, the molecule of **2a** features a different structure than the pseudo-tetrahedral geometry usually observed for related cyclopentadienyl− and indenyl−amido constrained-geometry yttrium and scandium complexes.[2,5b] The formal 14-electron yttrium center is coordinated in a distorted-octahedral fashion by the trimethylsilylmethyl ligand, *two* THF molecules, and the chelating amido and fluorenyl moieties, which are bonded in a dissymmetric $\eta^3$ fashion (Figure 1). The presence of an additional THF molecule in **2a**, as compared to monosolvated complexes $(\eta^5{:}\eta^1\text{-}C_5Me_4SiMe_2N^tBu)Y(CH_2SiMe_3)(THF)$ and $(\eta^5{:}\eta^1\text{-}C_9H_6SiMe_2N^tBu)Y(CH_2SiMe_3)(THF)$,[5b] is apparently directly connected to the reduced hapticity of the fluorenyl ligand.

(17) In contrast to amine elimination reactions involving bulky silylene-bridged bis(indenyl) ligands,[16c] it seems unlikely that the exchange reactions of lanthanide amides with our ligands could be hampered by the steric bulkiness of the reagents.

(18) Considering the even higher thermal instability of $La(CH(SiMe_3)_2)_3$,[6a] σ-bond metathesis between this reagent and **1a** was not attempted. Coordination of **1a** to larger lanthanides (La, Nd) was investigated using salt metathesis routes.

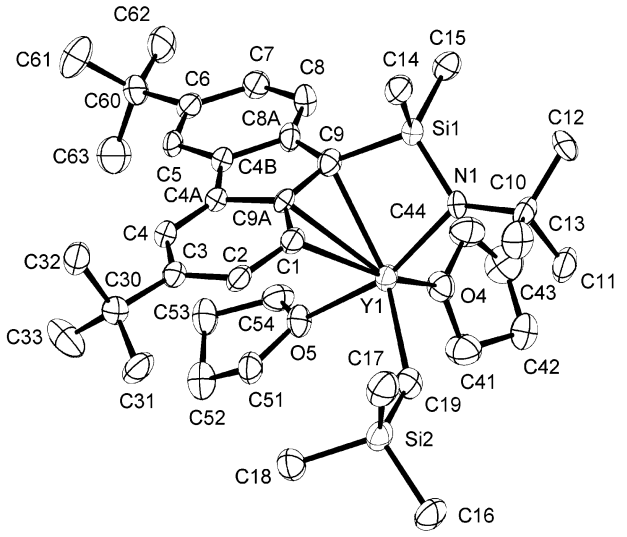


**Figure 1.** Molecular structure of complex **2a**. Thermal ellipsoids are drawn at the 50% probability level; hydrogen atoms are omitted for clarity. Selected bond distances (Å) and angles (deg): Y(1)−C(9), 2.584(7); Y(1)−C(9A), 2.732(7); Y(1)−C(1), 2.885(8); Y(1)−N(1), 2.200(6); Y(1)−C(19), 2.391(8); Y(1)−O(4), 2.322(5); Y(1)−O(5), 2.378(5); N(1)−Y(1)−C(9), 70.5(2); N(1)−Y(1)−C(9A), 88.5(2); N(1)−Y(1)−C(19), 107.8(2); N(1)−Y(1)−O(4), 94.9(2); N(1)−Y(1)−O(5), 158.5(2); C(19)−Y(1)−C(9), 148.2(3).

**Chart 1. Bonding Modes of the Fluorenyl Moieties Observed in Group 3 and Group 4 Metallocenes**

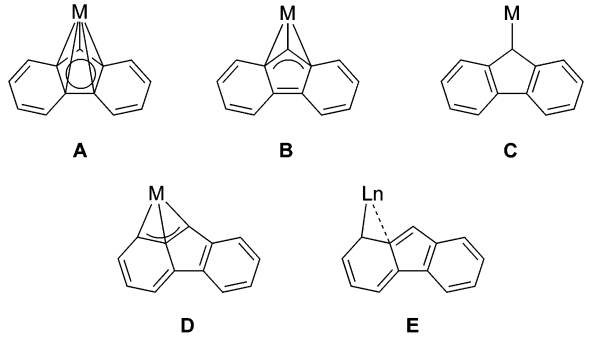


The bonding of the fluorenyl moiety in **2a** is unusual. Chart 1 shows various bonding modes of fluorenyl ligands found in ansa and simple metallocenes of lanthanides and zirconium previously established by X-ray diffraction studies.[19] In most complexes the metal is essentially symmetrically $\eta^5$ bonded to the five-membered ring of the fluorenyl ligand (**A**), e.g. in ($\eta^5$:$\eta^5$-CpSiMe$_2$Flu)Y[N(SiMe$_3$)$_2$],[14a] $\eta^3$ bonded (**B**), e.g. in ($\eta^5$:$\eta^3$-Flu)$_2$Sm(THF)$_2$[20] and ($\eta^5$:$\eta^3$-CpSiMe$_2$Flu)YCl$_2$-Li(OEt$_2$)$_2$,[14a] or, more seldomly, symmetrically $\eta^1$ bonded (**C**) as in ($\eta^5$-C$_5$H$_4$Me)$_2$Zr($\eta^1$-Flu)(Cl).[21] An unusual non-symmetric $\eta^3$-allyl bonding mode (**D**) involving the bridgehead carbon atom of the central ring and the two adjacent carbon atoms of one six-membered ring has been presented by Bochmann et al. in [($\eta^5$:$\eta^3$-CpCMe$_2$-Flu)Zr($\mu$-H)(Cl)]$_2$, with Zr−C(Flu) bond distances in the range 2.608(3)−2.686(3) Å.[22,23] Recently, we have reported a similar exocyclic $\eta^3$ bonding mode, together with a new exocyclic $\eta^1$($\eta^2$) bonding mode (**E**), in the unique, three polymorphic anion complex [($\eta^3$:$\eta^5$-FluCMe$_2$-Cp)($\eta^1$:$\eta^5$-FluCMe$_2$Cp)Y]$^-$[Li(Et$_2$O)(THF)$_3$]$^+$, with Y−C(1) in the range 2.690(7)−2.789(12) Å, Y−C(9A) in the range 2.749(7)−2.806(8) Å, and Y−C(9) in the range 2.894(8)−3.065(8) Å.[24] Complex **2a** features the same $\eta^3$-allyl bonding mode (**D**), slipped more toward the central five-membered ring than the six-membered ring, with Y(1)−C(9) = 2.584(7), Y(1)−C(9A) = 2.732(7) Å, and Y(1)−C(1) = 2.885(8) Å. The distance between the metal center and the bridgehead carbon atom C(9) of the central ring falls in the range for the Y−Cp(Flu) bond lengths of 2.56(2)−2.74(2) Å observed in ($\eta^5$:$\eta^5$-CpSiMe$_2$Flu)Y(N(SiMe$_3$)$_2$) and ($\eta^5$:$\eta^3$-CpSiMe$_2$Flu)YCl$_2$-Li(OEt$_2$)$_2$.[14a] Because of the dissymmetric coordination of the fluorenyl ligand, the bite angles in **2a** cannot be discussed as they usually can with Cp centroids. Nonetheless, the relevant bond angles Si(1)−N(1)−Y(1) (102.5(3)°) and N(1)−Si(1)−C(9) (101.5(3)°) resemble the corresponding angles in ($\eta^5$:$\eta^1$-C$_5$Me$_4$SiMe$_2$NCMe$_2$Et)Y(CH$_2$SiMe$_3$)(THF) (102.2(2) and 97.0(3)°)[5b] and [($\eta^5$:$\eta^1$-C$_5$Me$_4$SiMe$_2$NCMe$_2$R)Y(THF)($\mu$-Cl)]$_2$ (104.2(2) and 97.4°),[5c] which suggests comparable chelate constraints. Also, other bond distances associated to the carbyl, amido, and THF ligands in **2a** are similar to those found in (C$_5$Me$_4$SiMe$_2$NCMe$_2$Et)Y(CH$_2$SiMe$_3$)(THF).[5b]

Complex **2a** is readily soluble in aliphatic and aromatic hydrocarbons such as pentane, benzene, and toluene. The low-temperature (−70 °C) $^1$H NMR spectrum (toluene-$d_8$) of **2a** contains two singlets and four doublets characteristic for the six fluorenyl protons, two broad doublets for the diastereotopic C*HH*SiMe$_3$ protons ($^2J_{HH}$ = ca. 8 Hz), two singlets for the SiMe$_2$ moiety, two well-separated signals for the α-CH$_2$ THF protons, and one broadened signal for the $\beta$-CH$_2$ THF protons and each of the $^t$Bu (fluorene), $^t$Bu (amido), and SiMe$_3$ groups (Figure 2). This pattern indicates an asymmetric coordination sphere around yttrium and is consistent with a fixed distorted-octahedral geometry similar to that observed in the solid state for the bis(THF) complex (Figure 1). It suggests that reduced haptacity ($\eta^3$) of the fluorenyl moiety in **2a** is retained in solution; however, the NMR data provide no conclusive evidence about the exact bonding mode, i.e., symmetric (**B**) or dissymmetric (**D**).[25] As the temperature is raised from −70 °C to room temperature, the pairs of fluorenyl, C*HH*SiMe$_3$, SiMe$_2$, and α-CH$_2$ THF $^1$H NMR resonances of **2a** each broaden and collapse to a single resonance ($T_{coal}$ for C*HH*SiMe$_3$ is −35 °C at 300 MHz; $\Delta G^{\ddagger}_{coal}$ = 11.3 kcal/mol). The $^1$H NMR spectrum of **2a** in benzene or toluene at 20 °C

(19) Arene type $\eta^6$ coordination of fluorenyl ligands by the six-membered rings has been also observed in the solid state. (a) Bimetallic lanthanide−aluminum complexes [($\eta^6$-Me$_3$Si-fluorene)AlMe$_3$]$_2$Sm and [($\eta^6$-Me$_3$Si-fluorene)AlMe$_3$]Sm[$\eta^5$-Me$_3$Si-fluorenyl]: Nakamura, H.; Nakayama, Y.; Yasuda, H.; Maruo, T.; Kanehisha, N.; Kai, Y. *Organometallics* **2000**, *19*, 5392. (b) Fluorenyllithium ($\eta^6$-FluLi)$_2$: Üffing, C.; Köppe, R.; Schnöckel, H. *Organometallics* **1998**, *17*, 3512.

(20) Evans, W. J.; Gummersheimer, T. S.; Boyle, T. J.; Ziller, J. W. *Organometallics* **1994**, *13*, 1281.

(21) Schmid, M. A.; Alt, H. G.; Milius, W. *J. Organomet. Chem.* **1997**, *541*, 3.

(22) Bochmann, M.; Lancaster, S. J.; Hursthouse, M. B.; Mazid, M. *Organometallics* **1993**, *12*, 4718.

(23) A similar exocyclic $\eta^3$ coordination of fluorenyl ligands has been observed in the solid-state structures of alkaline-earth-metal complexes ($\eta^3$:$\eta^3$-FluSiMe$_2$Flu)$_2$M(THF)$_n$ (M = Ca, $n$ = 3; M = Ba, $n$ = 4): Harder, S.; Lutz, M.; Straub, W. G. *Organometallics* **1997**, *16*, 107.

(24) Kirillov, E.; Toupet, L.; Razavi, A.; Kahlal, S.; Saillard, J.-Y.; Carpentier, J.-F. *Organometallics* **2003**, *22*, 4038.

(25) In contrast to Bochmann's complex [($\eta^5$:$\eta^3$-CpCMe$_2$Flu)Zr($\mu$-H)(Cl)]$_2$,[22] in which the dissymmetry of the molecule observed by NMR in solution is clearly indicative of a dissymmetric bonding of the fluorenyl moiety, the dissymmetry of the molecule of **2a** is determined by the overall octahedral geometry, irrespective of the bonding mode of the fluorenyl group to the metal center.

Downloaded by CARLI CONSORTIUM on June 29, 2009
Published on September 30, 2003 on http://pubs.acs.org | doi: 10.1021/om0304210

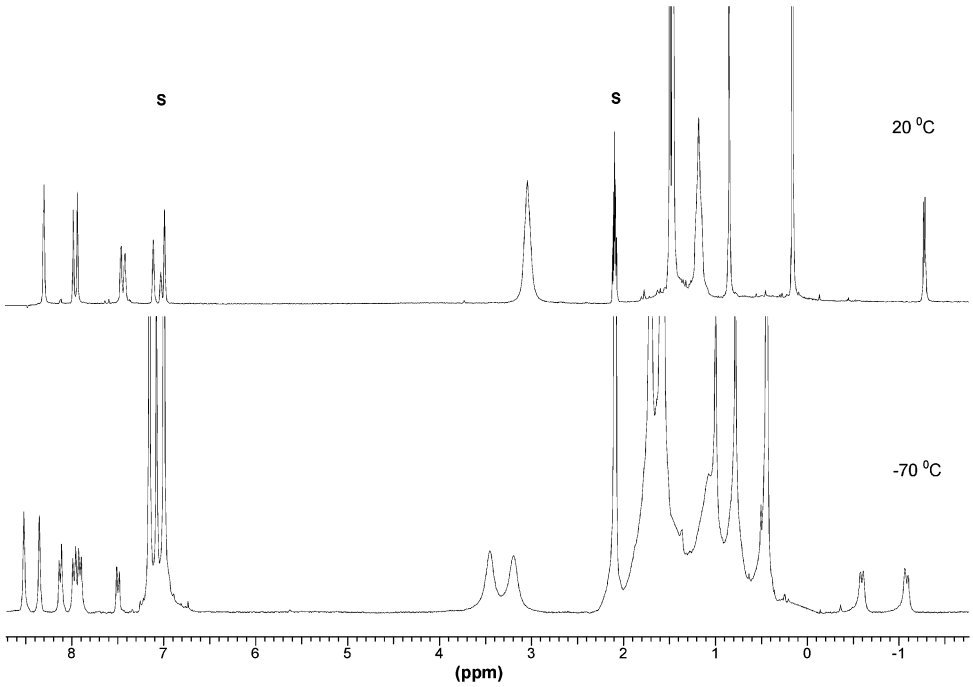


**Figure 2.** Temperature dependence of the $^1$H NMR spectrum of **2a** in toluene-$d_8$ (S denotes solvent resonances).

Downloaded by CARLI CONSORTIUM on June 29, 2009
Published on September 30, 2003 on http://pubs.acs.org | doi: 10.1021/om0304210

features one series of sharp signals, consistent with a symmetric structure on the NMR time scale (Figure 2). These line-shape changes are all reversible upon lowering the temperature. Also, the $^{13}C\{^1H\}$ NMR spectrum ($C_6D_6$) at 20 °C shows seven resonances for the fluorenyl carbon atoms, two signals for the THF carbons, one signal for the $SiMe_2$ bridge, and one doublet for the methylene carbon of the carbyl ligand ($^2J_{YH} = 3.3$ Hz). The coordinated THF ligands in **2a** are labile on the NMR time scale, as indicated by the temperature dependence of the chemical shifts of the α- and β-methylene THF protons, which undergo substantial low-field shifts when the temperature is raised from −30 to 60 °C (Figure 3). Addition of excess THF-$d_8$ resulted in the immediate exchange of all coordinated THF. These observations are in agreement with the existence of an equilibrium involving THF dissociation (eq 3), fast on

$$\underset{\textbf{2a}}{[(3,6\text{-}^t\mathrm{Bu}_2\mathrm{C}_{13}\mathrm{H}_6)\mathrm{SiMe}_2\mathrm{N}^t\mathrm{Bu}]\mathrm{Y}(\mathrm{CH}_2\mathrm{SiMe}_3)(\mathrm{THF})_2} \underset{+\mathrm{THF}}{\overset{-\mathrm{THF}}{\rightleftharpoons}} \underset{\textbf{2a}'}{[(3,6\text{-}^t\mathrm{Bu}_2\mathrm{C}_{13}\mathrm{H}_6)\mathrm{SiMe}_2\mathrm{N}^t\mathrm{Bu}]\mathrm{Y}(\mathrm{CH}_2\mathrm{SiMe}_3)(\mathrm{THF})} \quad (3)$$

both the chemical and NMR time scales.[5b] It is noteworthy that neither pumping of solid **2a** under high vacuum for prolonged periods nor repeated stripping of toluene solutions of **2a** yielded the monosolvated complex (**2a′**), suggesting that THF coordination is rather strong.

The diphenylsilylene-bridged ligand **1b** was found to be quite less reactive toward $Y(CH_2SiMe_3)_3(THF)_2$ than its dimethylsilylene analogue **1a**. $^1$H NMR monitoring of a 1:1 mixture in toluene-$d_8$ showed that no reaction occurs at 20 °C for several days. Heating at 50 °C for 2 days resulted in the formation of $[(3,6\text{-}^t\mathrm{Bu}_2\mathrm{C}_{13}\mathrm{H}_6)\mathrm{SiPh}_2\text{-}\mathrm{N}^t\mathrm{Bu}]\mathrm{Y}(\mathrm{CH}_2\mathrm{SiMe}_3)(\mathrm{THF})_x$ (**2b**) in 25% NMR yield (vs **1b**) and full decomposition of the starting yttrium carbyl (eq 2). On using an excess of $Y(CH_2SiMe_3)_3(THF)_2$ vs **1b** (4:1 ratio), the NMR yield of **2b** reached a maximum

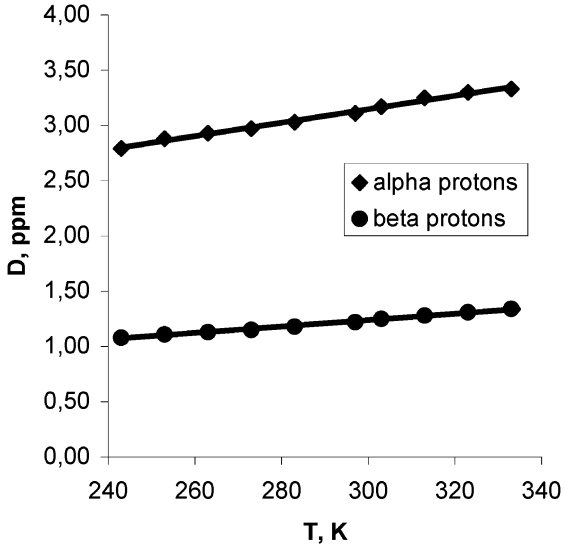


**Figure 3.** Temperature dependence of the chemical shift of the α- and β-$CH_2$ protons of the coordinated THF molecules in **2a** in toluene-$d_8$.

at 38% (vs **1b**) after 96 h at 50 °C; however, the reaction mixture was soiled by excess THF and insoluble decomposition products arising from the yttrium carbyl reagent, and this procedure proved to be inoperative on a larger scale to isolate pure carbyl complex **2b**. Also, significant decomposition of **2b** was observed at this temperature over several hours.

**Hydrogenolysis of Carbyl Complex 2a.** Numerous lanthanide hydrido complexes are described in the literature,[26] including a number of half-sandwich hydrido complexes derived from cyclopentadienyl−amido systems.[5a−c,9] However, to our knowledge, no fluorenyl hydrido complex of group 3 metals has been reported

(26) (a) Ephritikhine, M. *Chem. Rev.* **1997**, *97*, 2193. (b) Desurmont, G.; Li, Y.; Yasuda, H.; Maruo, T.; Kanehisa, N.; Kai, Y. *Organometallics* **2000**, *19*, 1811.

**Scheme 1. Putative Dimeric Hydrido Structures for the Hydrogenolysis Product of 2a**

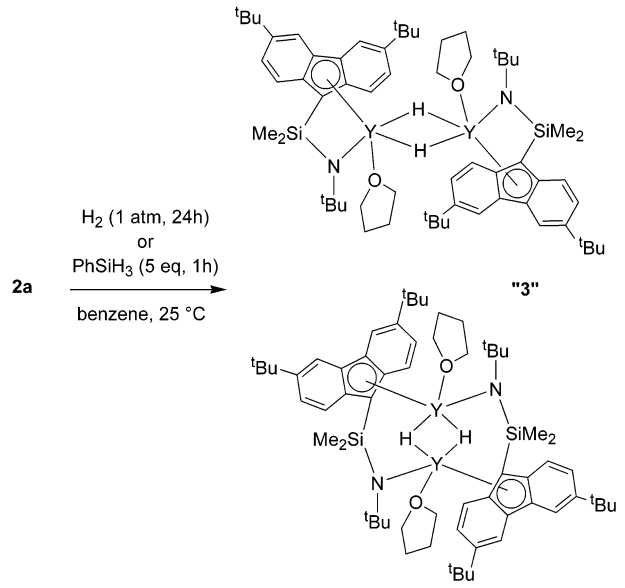


so far. Hydrogenolysis of **2a** in benzene (20 °C, 1 atm) proceeds smoothly with precipitation of a microcrystalline pale yellow powder (**3**) and concomitant production of $SiMe_4$ ($^1$H NMR). The same compound was obtained in nearly quantitative yield upon reacting **2a** and $PhSiH_3$ (5 equiv) in benzene solution at 20 °C for 1 h. This convergent reactivity of carbyl complex **2a** with both of the reagents traditionally used to prepare early-transition-metal hydrides[5a−c,9] and elemental analyses are in agreement with the formation of a hydrido complex of the proposed dimeric composition "[(3,6-$^t$Bu$_2$-Flu)SiMe$_2$N$^t$Bu)YH(THF)]$_2$" (**3**) (Scheme 1). This product is, however, totally insoluble in THF, DME, methylene chloride, and hydrocarbons (pentane, benzene, toluene), hampering recrystallization and NMR characterization.[27]

**Salt Elimination Reactions.** Salt elimination reactions between lanthanide halogenides $LnX_3$ (X = Cl, Br, I) and 1 equiv of deprotonated ligand salts $[L]^{2-}$ (L = e.g. bis(cyclopentadienyl), cyclopentadienyl−amido ligands) is usually carried out to access neutral or ate halogeno complexes of larger lanthanides of the type $\{[L]LnX\}_n$ ($n$ = 1, 2) and $\{[L]LnX_2\}^-$.[1] The latter can be then further transformed into potentially valuable carbyl or amido complexes. Such salt elimination reactions are most often performed in ethereal media ($Et_2O$, DME) to ensure solubility of the initial reagents and promote precipitation of the formed alkali-metal halide salts. Deprotonation of ligand **1a** is readily achieved with 2 equiv of $^n$BuLi (eq 4). The corresponding dilithium salt **4** is, however, extremely reactive toward protic sources, and its isolation, handling, and characterization are very arduous. X-ray-quality crystals of **4** were successfully grown from a THF/toluene solution (Figure 4, Table 1). On the other hand, attempts to characterize **4** by NMR in THF-$d_8$ solution systematically resulted in complicated spectra. The presence of a partially protonated species, i.e., the monolithiated derivative **5**, was suspected, likely due to adventitious hydrolysis with trace amounts of protic compounds in solvents or on glassware. Compound **5** was independently prepared by the reaction of **1a** with 1 equiv of $^n$BuLi in DME and recrystallized from a DME/pentane solution (eq 5). Again, no conclusive information was obtained in solution (NMR), but the solid-state characterization proved successful (Figure 5, Table 1).

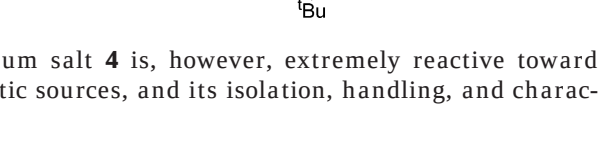


(4)

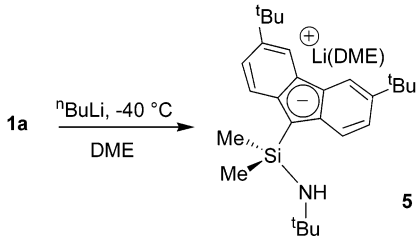


(5)

The solid-state structure of **4** features a "neutral" tris-THF solvate, unlike several dilithium salts of *ansa*-bis(fluorenyl) ligands which are presented by solvent-separated ion pairs, e.g. $[Me_2Si(Flu)_2Li(THF)_2]^-[Li(THF)_4]^+$ (**I**),[23] $[(CH_2)_n(Flu)_2Li]^-[Li(THF)_4]^+$ ($n$ = 2, 6),[28] and $[\{Flu(Me_2N)B-B(NMe_2)Flu\}Li(THF)]^-[Li(THF)_4]^+$.[29] The unit cell of **4** contains two independent molecules with similar geometries of the coordinated fluorenyl−amido moieties. The "amido" lithium atom Li(1) is in a three-coordinate planar environment (sum of the bond angles around Li(1) 357.4 and 355.9° in the two independent molecules), and the coordination environment of the "fluorenyl" lithium atom Li(2) is pseudo-tetrahedral. Interestingly, both lithium atoms are bonded to the nitrogen atom (Li(1)−N = 1.974(6) and 1.969(6) Å, Li(2)−N = 2.002(5) and 2.019(6) Å in the two independent molecules) and bridged by a THF molecule to give a nonplanar Li(1)−O(21)−Li(2)−N(1) core. Likewise, in $[Me_2Si(Flu)_2Li(THF)_2]^-[Li(THF)_4]^+$,[23] the lithium atom Li(2) in **4** is bonded to the fluorenyl group in an $\eta^1$ fashion with a fluorenyl $C_{ipso}$−Li bond distance (2.396(6) and 2.446(6) Å) comparable to those found in the former *ansa*-bis(fluorenyl) compound (2.353(8) and 2.399(8) Å).

The coordination in monolithiated species **5** is different. The fluorenyl group is $\eta^5$ bonded to lithium via the five-membered ring with Li−C bond distances in the range 2.291(5)−2.375(5) Å. A DME molecule completes the coordination sphere of the three-coordinate lithium atom, and the nitrogen atom of the pendant amino group is still protonated. This evidences the higher acidity of the fluorene functionality vs the amino moiety (vide supra).

(27) Recently we prepared the new hydrido complex $[(CpCMe_2Flu)Y(THF)(\mu\text{-}H)]_2$, which was shown by X-ray diffraction to be dimeric in the solid state and which features also extremely low solubility in most usual solvents: Kirillov, E.; Toupet, L.; Razavi, A.; Lehmann, C. W.; Carpentier, J.-F. Manuscript in preparation.

(28) Becker, B.; Enkelmann, V.; Mullen, K. *Angew. Chem., Int. Ed. Engl.* **1989**, *28*, 458.

(29) Littger, R.; Metzler, N.; Noth, H.; Wagner, M. *Chem. Ber.* **1994**, *27*, 1901.

Downloaded by CARLI CONSORTIUM on June 29, 2009
Published on September 30, 2003 on http://pubs.acs.org | doi: 10.1021/om0304210

Downloaded by CARLI CONSORTIUM on June 29, 2009
Published on September 30, 2003 on http://pubs.acs.org | doi: 10.1021/om0304210

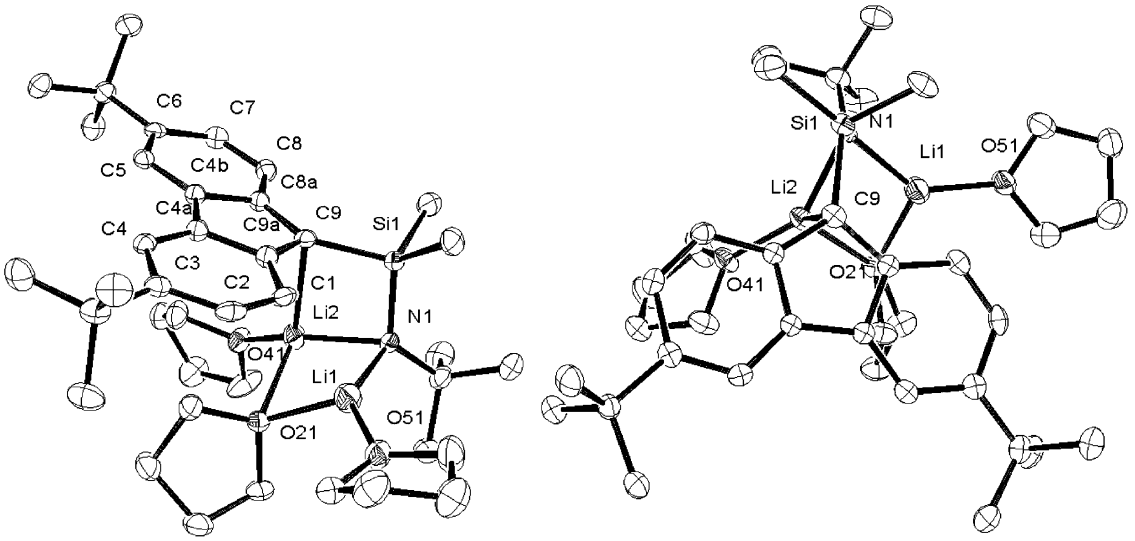


**Figure 4.** Molecular structure of $[(3,6\text{-}^{t}Bu_2C_{13}H_6)SiMe_2N^{t}Bu]Li_2(THF)_3\cdot 0.5C_7H_8$ (**4**). Two views and parameters of one of the two independent molecules are given; thermal ellipsoids are drawn at the 50% probability level, and hydrogen atoms are omitted for clarity. Selected bond distances (Å) and angles (deg): Li(1)−N(1), 1.974(6); Li(1)−O(21), 1.971(6); Li(1)−O(51), 1.901(6); Li(2)−C(9), 2.396(6); Li(2)−C(9a), 2.896(6); Li(2)−N(1), 2.002(5); Li(2)−O(21), 2.190(5); Li(2)−O(41), 1.915-(5); N(1)−Si(1)−C(9), 103.50(12); N(1)−Si(1)−Li(2), 47.37(13); C(9)−Si(1)−Li(2), 59.69(14); Li(1)−N(1)−Li(2), 77.8(2); Si(1)−N(1)−Li(1), 109.0(2).

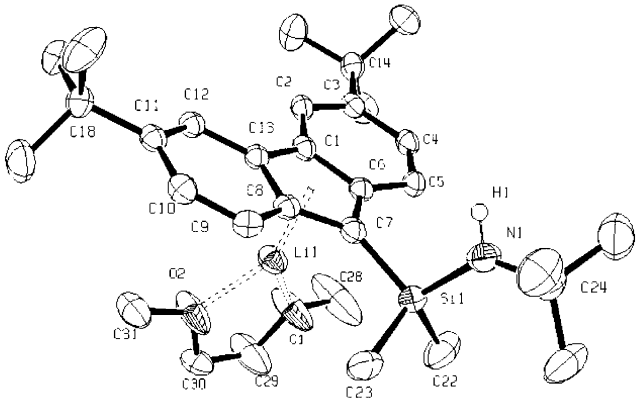


**Figure 5.** Molecular structure of $[(3,6\text{-}^{t}Bu_2C_{13}H_6)SiMe_2\text{-}NH^{t}Bu]Li(DME)$ (**5**). Thermal ellipsoids are drawn at the 50% probability level; hydrogen atoms, except that on the N atom, are omitted for clarity. Selected bond distances (Å) and angles (deg): Li(1)−O(1), 1.939(5); Li(1)−O(2), 1.927(5); Li(1)−C(1), 2.342(5); Li(1)−C(6), 2.304(5); Li(1)−C(7), 2.291(5); Li(1)−C(8), 2.336(5); Li(1)−C(13), 2.375(5); Cent−Li, 1.982; N(1)−Si(1)−C(7), 107.15(12); Si(1)−C(7)−Li(1), 118.67(17); Cent−Li(1)−O(1), 139.73; Cent−Li(1)−O(2), 137.31 Cent is the centroid of C(1)−C(6)−C(7)−C(8)−C(13).

Considering the high sensitivity of dilithiated ligand **4**, the latter was generated in situ just prior to salt metathesis reactions with $LnCl_3(THF)_n$ precursors. The first experiments were conducted with yttrium and lanthanum chlorides, since valuable NMR information is readily accessible for complexes of these diamagnetic metals and allows a thorough investigation of the reaction process. When carried out at room temperature in diethyl ether as the solvent, salt elimination from $YCl_3(THF)_{3.5}$ and $LaCl_3(THF)_{1.5}$ with 1 equiv of **4** gave crude products as yellow microcrystalline powders. The latter are only sparingly soluble in benzene and toluene and highly soluble in $Et_2O$, THF, and DME, suggesting an ionic structure. The $^1H$ and $^{13}C$ NMR spectra in THF-$d_8$ of both the Y and La crude products showed the presence of two major products (accounting for >95% of the sample) in comparable proportion (Y, 1.4:1; La, 1.2:1), which each feature one set of sharp resonances for a $[(3,6\text{-}^{t}Bu_2C_{13}H_6)SiMe_2N^{t}Bu]$ moiety symmetrically coordinated to the metal center on the NMR time scale. No change in the intensity ratio or broadening of the $^1H$ NMR signals was observed upon heating to 60 °C, indicating that no isomerization nor exchange takes place between these species under such conditions. Elemental analysis of both Y and La crude products did not match with calculated values for various formulas, confirming a mixture composition. Okuda et al. have reported that the reaction of $YCl_3(THF)_{3.5}$ with 1 equiv of $[C_5Me_4SiMe_2NCH_2CH_2OMe]Li_2$ in toluene or THF resulted in complex mixtures of inseparable products;[10a] only the reaction of anhydrous $LnCl_3$ (Ln = Y, Lu) with 2 equiv of $[C_5Me_4SiMe_2NCH_2CH_2X]Li_2$ (X = OMe, $NMe_2$) in THF afforded the isolable ionic bis(ligand) complexes $Li[Ln(\eta^5:\eta^1\text{-}C_5R_4SiMe_2NCH_2CH_2X)_2]$.[10a] Recrystallization of our crude 1:1 products proved more successful, leading reproducibly to a set of anionic complexes (eq 6).

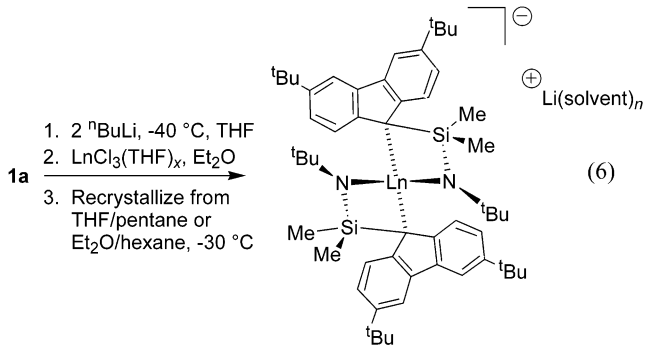


(6)

**6**: Ln = Y, solvent = THF, $n$ = 4 25% yield
**7**: Ln = La, solvent = THF, $n$ = 4 81% yield
**8**: Ln = La, solvent = $Et_2O$, $n$ = 2 33% yield

Recrystallization of the Y and La crude products from

Downloaded by CARLI CONSORTIUM on June 29, 2009
Published on September 30, 2003 on http://pubs.acs.org | doi: 10.1021/om0304210

THF/pentane at −30 °C gave yellow crystals of the ionic complexes $[\{(3,6\text{-}^tBu_2C_{13}H_6)SiMe_2N^tBu\}_2Ln]^-[Li(THF)_4]^+$ (Ln = Y, **6**; Ln = La, **7**) in 25% and 81% yields (vs **1a**), respectively. Elemental analyses were in agreement with the proposed formulas for complexes **6** and **7**, indicating in particular that there is essentially no Cl. The isolated complexes show the same solubility trend as the initial crude products: that is, quite poor solubility in hydrocarbons and high solubility in ether solvents. In fact, $^1H$ and $^{13}C$ NMR spectroscopy established unambiguously that complex **7** corresponds to the initially minor species present in the crude La product. On the other hand, the $^1H$ NMR spectrum of **6** in THF-$d_8$ at 20 °C displays one set of sharp signals characteristic of a symmetrically coordinated $[(3,6\text{-}^tBu_2C_{13}H_6)SiMe_2N^tBu]$, yet the chemical shifts are significantly different from those of both species present in the crude Y product. The identity of the latter thus still remains obscure. Although no crystal of **6** or **7** suitable for X-ray diffraction studies could be obtained, the molecular structure of a close neodymium parent complex (**9**) was further established (vide infra).

Recrystallization of the crude La product (obtained from $LaCl_3(THF)_{1.5}$ and in situ generated **4** in $Et_2O$) under different conditions, i.e., from an $Et_2O$/hexane mixture, afforded the ionic compound $[\{(3,6\text{-}^tBu_2C_{13}H_6)SiMe_2N^tBu\}_2La]^-[Li(Et_2O)_2]^+$ (**8**) as orange-yellow crystals in 33% yield (vs **1a**). Complex **8** is sparingly soluble in toluene and highly soluble in THF and diethyl ether, consistent with its ionic structure. The $^1H$ NMR spectrum of **8** at 20 °C in THF-$d_8$ (as well as that in toluene-$d_8$) displays broad signals indicative of a fluxional behavior and does not correspond to either of the two sets of resonances observed for the initial crude La product. Fast exchange on the NMR time scale occurs when the temperature is raised to 60 °C, with the characteristic pattern of sharp resonances for a symmetrically coordinated $[(3,6\text{-}^tBu_2C_{13}H_6)SiMe_2N^tBu]$ moiety.

An X-ray diffraction study confirmed the nature of **8** (Figure 6, Table 1). The solid-state molecular structure features a closely associated ion pair with two chelating ligands per lanthanum center, and this fragment is therefore anionic. The counterion is characterized by a lithium atom coordinated in a pseudo-tetrahedral fashion by two diethyl ether molecules and two carbon atoms of the central five-membered ring (C(7) and C(8)) of one fluorenyl moiety. The formal 16-electron lanthanum atom is coordinated in a distorted-tetrahedral geometry by a pair of amido and fluorenyl moieties. Each of the latter is coordinated in an $\eta^3$ fashion involving the bridgehead carbon atom of the central five-membered ring (C(7) and C(28)) and the two adjacent carbon atoms fusing the five- and six-membered rings (C(6), C(8) and C(27), C(29)). The $\eta^3$ coordination mode of the two fluorenyl ligands is, however, not as symmetric as in the ideal case (**B**, Chart 1). The La atom is slipped on one side of the fluorenyl system, resulting in a ca. 0.2 Å difference between the bond distances of La with the two terminus carbon atoms (C(6), C(8) and C(27), C(29)), a deviation likely attributable to the chelating constraints imposed by the silylene bridge or crystal packing. The La−C(Flu) bond distances are somewhat different in both fluorenyl rings, since one of the latter

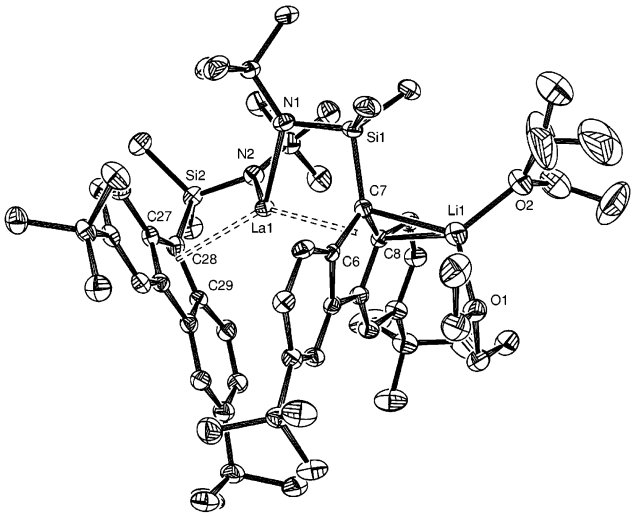


**Figure 6.** Molecular structure of **8**. Thermal ellipsoids are drawn at the 50% probability level; hydrogen atoms are omitted for clarity. Selected bond distances (Å) and angles (deg): La(1)−C(6), 3.025(4); La(1)−C(7), 2.806(4); La(1)−C(8), 2.883(4); La(1)−C(27), 2.843(4); La(1)−C(28), 2.766(4); La(1)−C(29), 3.068(4); Li(1)−C(7), 2.279(9); La(1)−N(1), 2.396(3); La(1)−N(2), 2.378(3); Li(1)−C(8), 2.439(9); Li(1)−O(1), 1.919(9); Li(1)−O(2), 1.910(9); N(1)−La(1)−N(2), 101.76(12); Cent(1)−La(1)−N(1), 75.86; Cent(2)−La(1)−N(2), 76.38; C(7)−Si(1)−N(1), 101.01(17); C(28)−Si(2)−N(2), 100.84(17). Cent(1) is the centroid of C(6)−C(7)−C(8); Cent(2) is the centroid of C(27)−C(28)−C(29).

is also coordinated to the Li atom (2.806(4)−3.025(4) and 2.766(4)−3.068(4) Å) and are similar to those observed in $[(\eta^5\text{:}\eta^5\text{-}CpCPh_2Flu)La(BH_4)_2]^-[Li(THF)_4]^+$ (2.788(3)−3.010(3) Å)[14c] and in the chelated ring of $(\eta^5\text{:}\eta^5\text{-}CpCMe_2Flu)La(\eta^5\text{-}CpCMe_2FluH)(THF)$ (2.811(5)−2.997(6) Å).[14g] The La−N($^t$Bu) bond distances in **8** (2.378(3)−2.396(3) Å) fall in the same range as those observed in other related La−amido species; e.g., $La[CyNC(NSiMe_3)_2NCy][N(SiMe_3)_2]_2$ (2.377(3)−2.382(3) Å)[30] and $Cp^*_2La(NHMe)(H_2NMe)$ (2.323(10) Å).[31] These values are consistent with a $\pi$-dative interaction between the Lewis acidic La center with the free electron pair on nitrogen,[32] also indicated by the sp$^2$ hybridization of the N atoms (sum of the bond angles: around N(1), 359.9(1)°; around N(2), 360.0(1)°). This La−N($^t$Bu) distance is longer than that observed in $(\eta^5\text{:}\eta^1\text{-}C_5Me_4SiMe_2N^tBu)Sm[N(SiMe_3)_2]$ (2.257(4) Å),[6a] $(\eta^5\text{:}\eta^1\text{-}C_5Me_4SiMe_2NCMe_2Et)Y(CH_2SiMe_3)(THF)$ (2.208(6) Å),[5b] and $[\eta^5\text{:}\eta^1\text{-}(3,6\text{-}^tBu_2C_{13}H_6)SiMe_2N^tBu]ZrCl_2$ (2.040(8) Å),[15a] as expected from the major influence of effective ionic radii of the metal centers.[33] Complex **8** features very narrow bite angles. The angle $Flu_{Cent}$−La−N ($Flu_{Cent}$ and N of the same ligand; Cent(1)−La(1)−N(1) = 75.9° and Cent(2)−La(1)−N(2) = 76.4° considering centroids of C(6)−C(7)−C(8) and C(27)−C(28)−C(29), respectively; Cent′(1)−La(1)−N(1) = 85.2° considering a fluorenyl $C_5$ ring centroid) is much narrower than that observed in Li-

(30) Giesbrecht, G. R.; Whitener, G. D.; Arnold, J. *J. Chem. Soc., Dalton Trans.* **2001**, 923.
(31) Gagné, M. R.; Stern, C. L.; Marks, T. J. *J. Am. Chem. Soc.* **1992**, *114*, 275.
(32) Lauher, J. W.; Hoffmann, R. *J. Am. Chem. Soc.* **1976**, *98*, 1729.
(33) Effective ionic radii for eight-coordinate metal centers: $La^{3+}$, 1.160 Å; $Nd^{3+}$, 1.109 Å; $Sm^{3+}$, 1.079 Å; $Y^{3+}$, 1.019 Å; $Zr^{4+}$, 0.84 Å. Shannon, R. D. *Acta Crystallogr., Sect. A* **1976**, *A32*, 751.

**Scheme 2**

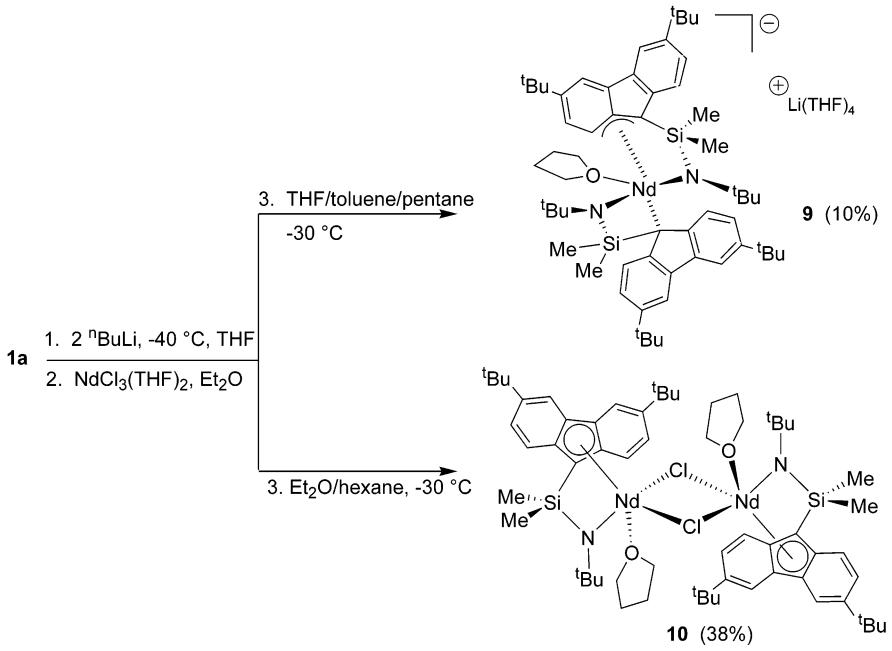


Downloaded by CARLI CONSORTIUM on June 29, 2009
Published on September 30, 2003 on http://pubs.acs.org | doi: 10.1021/om0304210

$[Y(\eta^5{:}\eta^1\text{-}C_5Me_4SiMe_2NCH_2CH_2OMe)_2]$ (95.7°)[10] and $[\eta^5{:}\eta^1\text{-}(3,6\text{-}^tBu_2C_{13}H_6)SiMe_2N^tBu]ZrCl_2$ (104.7°).[15a]

The same salt elimination synthetic approach was applied to neodymium chemistry (Scheme 2). Efficient purification procedures and corresponding X-ray structural information were crucial in this case, since complicated and usually uninformative NMR data are obtained for complexes of this paramagnetic metal. Thus, crystallization of the crude product obtained from the reaction of $NdCl_3(THF)_2$ with 1 equiv of dilithium salt **4** (generated in situ) in $Et_2O$ was attempted under different conditions. Crystallization from a THF/toluene/pentane solution gave in poor yield (10% vs **1a**) golden yellow crystals of $[\eta^3{:}\eta^1\text{-}\{(3,6\text{-}^tBu_2C_{13}H_6)SiMe_2N^tBu\}_2Nd(THF)]^-[Li(THF)_4]^+$ (**9**). The ionic complex **9** is the Nd homologue of Y and La complexes **6** and **7**, respectively. On the other hand, using a $Et_2O$/hexane solution allowed us to isolate green crystals of the *neutral* chloro complex $[\eta^5{:}\eta^1\text{-}\{(3,6\text{-}^tBu_2C_{13}H_6)SiMe_2N^tBu\}Nd(\mu\text{-}Cl)(THF)]_2$ (**10**) (38% vs Nd). The identity of **9** and **10** was unambiguously established by single-crystal X-ray diffraction studies (Figures 7 and 8, Table 1).

The molecular structure of **9** comprises a fully dissociated ion pair in the solid state. The cation is composed by a lithium atom coordinated by four THF molecules, as observed in other ionic lanthanidocenes.[14d-g] The neodymium atom is coordinated in a distorted-trigonal-bipyramidal geometry by one THF molecule and a pair of amido and fluorenyl moieties. In contrast with the anionic bis(ligand) lanthanum complex **8**, but similarly to neutral yttrium carbyl **2a**, both fluorenyl moieties in **9** are coordinated to Nd in a dissymmetric fashion. A clear dissymmetric $\eta^3$ bonding mode (**D**, Chart 1) is established for one fluorenyl ligand (C(28), C(29), C(30)), with Nd−C(Flu) bond distances in the range of 2.789(5)−3.017(5) Å. The corresponding Nd−C(Flu) bond distances of the second fluorenyl moiety are in the range of 2.710(5)−3.184(5) Å, with the phenyl carbon atom (C(3)) being farther away from the metal center. The difference of nearly 0.5 Å between the shortest and the longest bond distances indicates that this fluorenyl ring may be in a stage of approaching toward reduced hapticity ($\eta^2$ or $\eta^1$ bonding mode). This is consistent with a 16-electron count on the metal complex, equivalent to that of **8**, considering two-$\sigma$-electron donation from the coordinated THF.

On the other hand, neutral complex **10** shows in the solid state a dimeric $C_i$-symmetric structure. Each (equivalent) neodymium atom is coordinated by two bridging chlorine atoms, a THF molecule, and the amido and fluorenyl moieties of a chelating ligand. The structure can be regarded as the trans-heterochiral dimer, according to the classification in Chart 2.[34] The same diastereoselectivity in the crystal has been observed

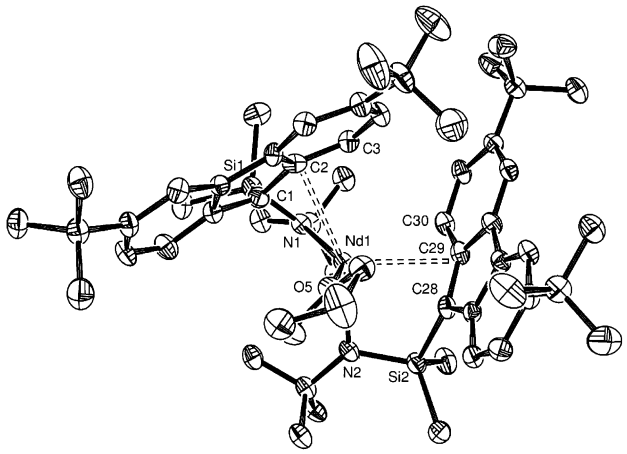


**Figure 7.** Molecular structure of the anion of **9**. Thermal ellipsoids are drawn at the 50% probability level; hydrogen atoms are omitted for clarity. Selected bond distances (Å) and angles (deg): Nd(1)−C(1), 2.710(5); Nd(1)−C(2), 3.068(5); Nd(1)−C(3), 3.184(5); Nd(1)−C(28), 2.789(5); Nd(1)−C(29), 2.901(5); Nd(1)−C(30), 3.017(5); Nd(1)−N(1), 2.353(4); Nd(1)−N(2), 2.298(4); Nd(1)−O(5), 2.522(3); N(1)−Nd(1)−N(2), 102.20(14); N(1)−Nd(1)−C(1), 67.87(14); N(1)−Nd(1)−C(2), 84.06(13); N(2)−Nd(1)−C(28), 66.53(14); N(2)−Nd(1)−C(29), 90.53(14); C(1)−Si(1)−N(1), 104.7(2); C(28)−Si(2)−N(2), 103.7(2).

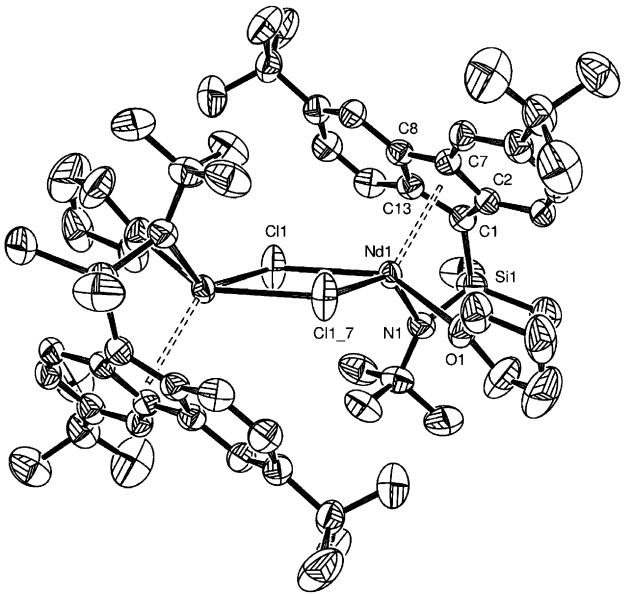


**Figure 8.** Molecular structure of **10**. Thermal ellipsoids are drawn at the 40% probability level; hydrogen atoms are omitted for clarity. Selected bond distances (Å) and angles (deg): Nd(1)−C(1), 2.646(3); Nd(1)−C(2), 2.801(3); Nd(1)−C(7), 2.900(4); Nd(1)−C(8), 2.862(4); Nd(1)−C(13), 2.709(4); Nd(1)−Cent, 2.502; Nd(1)−N(1), 2.259(3); Nd(1)−Cl(1), 2.7888(10); Nd(1)−Cl(1_7), 2.8622(10); Nd(1)−O(1), 2.493(3); Cent−Nd(1)−N(1), 94.13; Cent−Nd(1)−Cl(1), 127.87; Cent−Nd(1)−Cl(1_7), 110.15; Cl(1)−Nd(1)−N(1), 99.25(9); Cl(1)−Nd(1)−Cl(1_7), 74.05(3); O(1)−Nd(1)−N(1), 89.33(11). Cent is the centroid of C(1)−C(2)−C(7)−C(8)−C(13).

**Chart 2**

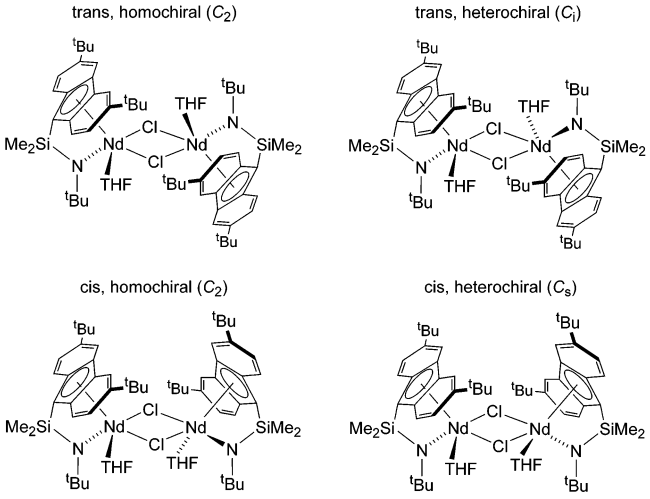


previously for the parent complex [Y($\eta^5$:$\eta^1$-$C_5Me_4SiMe_2$-$NCMe_2Et$)($\mu$-Cl)(THF)]$_2$[5c] and dimeric scandium hydride and carbyl complexes of the tridentate ligand $CpH^{NMe}$-$SiMe_2NH^tBu$.[9] The metrical features of the rhomboidal $Nd_2Cl_2$ core (Nd(1)−Cl(1) = 2.789(1) Å; Nd(1)−Cl(1_7) = 2.862(1) Å; Nd(1)−Cl(1)−Nd(1) = 105.95(3); Cl(1)−Nd(1)−Cl(1_7) = 74.05(3)°) indicate asymmetry in the chloride bridges[35] comparable to that observed in [Nd{$N(SiMe_3)_2$}$_2$(THF)($\mu$-Cl)]$_2$ (Nd−Cl = 2.791(3) and 2.854(3) Å; Nd−Cl−Nd = 106.3(1)°; Cl−Nd−Cl = 73.66(10)°),[36] [($\eta^5$-Cp)$_2$Nd(THF)($\mu$-Cl)]$_2$ (Nd−Cl = 2.787(4) and 2.861(4) Å; Nd−Cl−Nd = 106.3(1)°; Cl−Nd−Cl = 73.7(1)°)[37] and the aforementioned parent CGC yttrium complex.[5c] The fluorenyl moieties in **10** are $\eta^5$ coordinated to the central five-membered ring (mode **A**, Chart 1) with Nd−C(Flu) bond distances in the range of 2.646(3)−2.900(4) Å and average of 2.784(4) Å, a value smaller than the average bond distance of 2.845(4) Å in [($\eta^5$:$\eta^5$-$CpCPh_2Flu$)$Nd(BH_4)_2$]$^-$[$Li(THF)_4$]$^+$[14c] and 2.883(4) Å in ($\eta^5$:$\eta^5$-$CpCMe_2Flu$)Nd($\eta^5$-$CpCMe_2FluH$)(THF).[14g]

The Nd−N($^t$Bu) bond distances in **9** (2.298(4)−2.353(4) Å) are slightly shorter than those in the lanthanum complex **8**, reflecting the decrease by 4% in the ionic radii.[33] They compare well with the bond distances observed in other amido−neodymium complexes, e.g. [Nd{$N(SiMe_3)_2$}$_2$(THF)($\mu$-Cl)]$_2$ (2.300(8)−2.335(8) Å)[36] and $Nd[N(SiHMe_2)_2]_3(THF)_2$ (2.326(5)−2.353(5) Å),[30] while the distance in **10** (2.259(3) Å) is slightly shorter. As for **8**, these values are consistent with a $\pi$-dative interaction between the Lewis acidic Nd center with the free electron pair on nitrogen,[32] also indicated by the $sp^2$ hybridization of the N atoms (sum of the bond angles: around N(1) in **9**, 359.9(2)°; around N(2) in **9**, 359.9(2)°; around N(1) in **10**, 360.0(3)°). The bite angle $Flu_{Cent}$−Nd(1)−N(1) (94.13°) in the constrained-geometry complex **10** is much smaller than the $Flu_{Cent}$−Nd−$Cp_{cent}$ bite angle observed in [($\eta^5$:$\eta^5$-$CpCPh_2Flu$)Nd$(BH_4)_2$]$^-$[$Li(THF)_4$]$^+$ (ca. 106°)[14c] and ($\eta^5$:$\eta^5$-$CpCMe_2Flu$)-Nd($\eta^5$-$CpCMe_2FluH$)(THF) (105.08°)[14g] and even smaller than that in silylene-bridged bis(cyclopentadienyl)-Nd systems, e.g. {$Me_2Si(\eta^5$-$C_5Me_4)_2$}Nd[$CH(SiMe_3)_2$] (121.6°)[38] and [*rac*-{$Me_2Si(\eta^5$-2-$SiMe_3$-4-$^tBuC_5H_4)_2$}Nd-($\mu$-Cl)$_2$Li(THF)$_2$] (118.9°).[39]

All of the above results show that salt elimination reactions of lanthanide chlorides with 1 equiv of the dilithiated species of linked fluorenyl−amido ligand **1a** are quite versatile. Two classes of products are formed: homoleptic ionic complexes that contain two chelating ligand units per metal center (**A**)[40] and heteroleptic neutral chloro complexes with one chelating ligand unit (**B**). Only the major product isolated from neodymium chloride belongs to the latter (most preferred) class. The same selectivity for neutral chloro complexes of type **B** was described by Bercaw et al. in the chemistry of scandium constrained-geometry complexes.[2c] This is rather surprising, since the organometallic chemistry of Nd and Sc are known to be quite different,[1] in particular because of the large difference in the ionic radii of these elements.[33] On the other hand, yttrium and lanthanum, despite their large difference in ionic radius, both induce ionic species of type **A**. A few examples of formation of such ionic complexes that contain *two* chelating units per metal center in the course of *equimolar* salt metathesis reactions have been

(34) Von Zelewsky, A. *Stereochemistry of Coordination Compounds*; Wiley: Chichester, U.K., 1996; p 78.

(35) Other dimeric THF-free bis(cyclopentadienyl)neodymium chlorides exhibit more symmetric rhomboidal $Nd_2Cl_2$ cores. (a) [Nd($\eta^5$-$C_5H_4$-{$CH(SiMe_3)_2$})$_2$($\mu$-Cl)]$_2$ (Nd−Cl = 2.805(1), 2.786(1) Å; Nd−Cl−Nd = 103.24(3)°; Cl−Nd−Cl = 76.76(3)°): Hitchcock, P. B.; Lappert, M. F.; Tian, S. *Organometallics* **2000**, *19*, 3420. (b) [Nd(1,3-$^tBu_2C_5H_3$)$_2$($\mu$-Cl)]$_2$ (Nd−Cl = 2.837(1), 2.841(1) Å): Marks, T. J.; Grynkewich, G. W. *Inorg. Chem.* **1976**, *15*, 1302.

(36) Berg, D. J.; Gendron, R. A. L. *Can. J. Chem.* **2000**, *78*, 454.

(37) Jin, Z.; Liu, Y.; Chen, W. *Sci. Sin., Ser. B* **1987**, *1*, 1.

(38) Jeske, G.; Schock, L. E.; Swepston, P. N.; Schumann, H.; Marks, T. J. *J. Am. Chem. Soc.* **1985**, *107*, 8103.

(39) Bogaert, S.; Chenal, T.; Mortreux, A.; Nowogrocki, G.; Lehmann, C. W.; Carpentier, J.-F. *Organometallics* **2001**, *20*, 199.

(40) For the neutral parent complex ($\eta^5$:$\eta^1$-$C_5Me_4SiMe_2N^tBu$)Sm($\eta^5$-$C_5Me_4SiMe_2NH^tBu$), see ref 6a.

Downloaded by CARLI CONSORTIUM on June 29, 2009
Published on September 30, 2003 on http://pubs.acs.org | doi: 10.1021/om0304210

**Table 2. Polymerization of MMA Promoted by 2a, 3, and 10[a]**

| compd | conditions | temp, °C | yield, % | $10^3 M_w$[b] | $M_w/M_n$[b] | tacticity[c] mm | mr | rr |
|---|---|---|---|---|---|---|---|---|
| **2a** | toluene[d] | 20 | 2 | nd[e] | nd[e] | 42 | 29 | 29 |
| **2a** | | 50 | 2 | nd[e] | nd[e] | 40 | 29 | 32 |
| **3** | | 20 | 13 | 19 | 2.8 | 41 | 26 | 33 |
| **7** | bulk | 20 | 26 | 250 | 2.8 | 34 | 40 | 26 |
| **7** | | 50 | 65 | 216 | 3.6 | 39 | 40 | 21 |

[a] Conditions: [MMA]/[cat.] = 500; reaction time 12 h. [b] Average weight molecular mass and polydispersity as determined by GPC. [c] Determined by $^1$H NMR in $CDCl_3$. [d] As 0.5−1.0 M solutions. [e] PMMA not soluble in THF.

reported: e.g., $[Lu\{ArN(CH_2)_3NAr\}_2]^-[LuCl_2(THF)_5]^+$,[41] and $[(FluCMe_2Cp)_2Y]^-[Li(Et_2O)(THF)_3]^+$.[24] The mechanistic pathway for the formation of complexes **A** such as **6**−**9** remains unclear. Disproportionation of intermediary species of type **B** appears as the most likely hypothesis. However, in such cases, we see no obvious reason to account for the instability of the latter neutral chloro yttrium and lanthanum complexes as compared to the fairly stable neodymium product (**10**).

**Polymerization Activity of Fluorenyl-Based CGC.** Effective polymerization of ethylene and polar monomers, such as *tert*-butyl acrylate, with cyclopentadienyl−amido yttrium carbyl and hydride CGC has been reported by Okuda et al.[5a,c] We were therefore interested in evaluating the polymerization ability of some of the fluorenyl−amido complexes we prepared. Yttrium carbyl **2a** and its "hydrido" derivative **3** were found to be inactive toward ethylene in the temperature range 20−80 °C (1 atm of $C_2H_4$). The inactivity of **2a** likely arises from the initial presence of two THF molecules in the coordination sphere of yttrium, as compared to the active cyclopentadienyl analogue $(C_5Me_4SiMe_2N^tBu)Y(CH_2SiMe_3)(THF)$, which contains only one coordinated THF molecule.[5c] Despite the fact that the first THF molecule in **2a** dissociates rather quickly above room temperature (vide supra), the remaining THF ligand might block the "active site". Dimeric neodymium chloride **10**, when activated with 1 equiv of $LiCH(SiMe_3)_2$,[42] polymerizes ethylene with low activity (1.3 kg of PE/((mol of Nd) h atm) at 20 °C and 4 atm of $C_2H_4$) to yield polyethylene with $T_m$ = 134 °C, $M_n$ = 140 000, and $M_w/M_n$ = 2.46. Only traces of polyethylene were obtained on using the in situ combinations **10**/$Mg(^{n,s}Bu)_2$ (1:40)[39] and **10**/DIBALH/$^n$BuLi (1:20:20)[43] as catalyst systems under similar conditions. Also, modest performance was observed in the polymerization of MMA (Table 2). Quite surprisingly, anionic lanthanum complex **7** reacts smoothly with bulk MMA at room temperature and 50 °C to give high-molecular-weight atactic PMMA. The mechanism for MMA polymerization with this complex remains unclear and might involve initiation via insertion into either an La−fluorenyl or La−amido bond.[1i,44]

## Conclusion

In summary, we have shown that alkane elimination is a viable route toward new fluorenyl-based constrained-geometry carbyl complexes of yttrium. On the other hand, salt elimination reactions of yttrium and lanthanum chlorides with 1 equiv of the dilithiated species of linked fluorenyl−amido ligand **1a** lead to chlorine-free, ionic complexes that contain two chelating ligand units per metal center. The latter are likely formed by disproportionation of intermediary neutral chloro fluorenyl−amido complexes, a class of which only the neodymium complex could be isolated in valuable yield. One of the most striking features of these novel constrained-geometry complexes, in addition to their very narrow $Flu_{Cent}$−Ln−N bite angles, is the versatility of the coordination mode of the fluorenyl ligand observed in the solid state. In the four structurally characterized rare−earth complexes reported in this paper, at least three distinct bonding modes have been observed: $\eta^3$- and $\eta^5$-symmetric modes involving carbon atoms of the central Cp ring (**8**, **10**) and an unusual $\eta^3$-dissymmetric mode involving carbon atoms of the central Cp and one adjacent phenyl rings (**2a**, **9**). Reduced hapticity ($\eta^3$) of the fluorenyl moiety in the carbyl complex has been found to be associated with the coordination of extra donor solvent molecules (THF), as compared to analogous cyclopentadienyl−amido complexes, a phenomenon that might account for the poor catalytic performances observed in polymerization.

## Experimental Section

**General Procedures.** All manipulations were performed under a purified argon atmosphere using standard high-vacuum Schlenk techniques or in a glovebox. Solvents were freshly distilled from Na/benzophenone (THF, $Et_2O$, DME) and Na/K alloy (toluene, pentane) under nitrogen and degassed thoroughly by freeze−thaw−vacuum cycles prior to use. Deuterated solvents (benzene-$d_6$, toluene-$d_8$, THF-$d_8$; pyridine-$d_5$ >99.5% D, Eurisotop) were vacuum-transferred from Na/K alloy into storage tubes. $YCl_3(THF)_{3.5}$ and $LaCl_3(THF)_{1.5}$ were obtained after repeated extraction of $YCl_3$ and $LaCl_3$ (Strem) from THF. $NdCl_3(THF)_2$ was generously provided by Rhodia. $Y[N(SiHMe_2)_2]_3(THF)_2$,[30] $Ln[N(SiMe_3)_2]_3$ (Ln = Y, La),[14g] and $Y(CH_2SiMe_3)_3(THF)_2$[45] were prepared by following literature procedures. The ligands $(3,6\text{-}^tBu_2C_{13}H_7)SiR_2NH^tBu$ (R = Me, **1a**; R = Ph, **1b**) were provided by TotalFinaElf and recrystallized from pentane prior to use. NMR spectra were recorded on Bruker AC-200 and AC-300 spectrometers in Teflon-valved NMR tubes. $^1$H and $^{13}$C chemical shifts are reported in ppm vs $SiMe_4$ and were determined by reference to the residual solvent peaks. Assignment of signals was made from $^1$H−$^1$H COSY, $^1$H−$^{13}$C HMQC, and HMBC NMR experiments. Coupling constants are given in hertz. Elemental analyses were performed by the Microanalytical Laboratory at the Institute of Chemistry of Rennes and are the average of two independent determinations.

**$[\eta^3{:}\eta^1\text{-}(3,6\text{-}^tBu_2C_{13}H_6)SiMe_2N^tBu]Y(CH_2SiMe_3)(THF)_2$ (2a). (a) NMR-Scale Reaction.** An NMR tube was charged with $Y(CH_2SiMe_3)_3(THF)_2$ (32 mg, 0.065 mmol) and $3,6\text{-}^tBu_2C_{13}H_7SiMe_2NH^tBu$ (**1a**; 27 mg, 0.065 mmol). Benzene-$d_6$ (ca. 0.6 mL) was vacuum-transferred in at −196 °C, and the tube was warmed to room temperature. Progress of the reaction was monitored periodically by $^1$H NMR spectroscopy, which showed selective formation of **2a** (>98% vs ligand), with concomitant

(41) Roesky, P. W. *Organometallics* **2002**, *21*, 4756.

(42) Reaction of **10** and 1 equiv (vs Nd) of $LiCH(SiMe_3)_2$ in toluene at room temperature proceeded with precipitation of a white solid, assumed to be LiCl. Attempts to isolate analytically pure samples and to grow crystals suitable for X-ray diffraction of the putative hydrocarbyl complex $[(3,6\text{-}^tBu_2C_{13}H_6)SiMe_2N^tBu]Nd(CH(SiMe_3)_2)(THF)_x$ (red gummy solid) were unsuccessful.

(43) Boisson, C.; Barbotin, F.; Spitz, R. In *Progress and Development in Catalytic Olefin Polymerization*; Sano, T., Uozomi, T., Nakatani, H., Terano, M., Eds.; Technology and Education Publishers: Tokyo, 2000; p 75.

(44) Giardello, M. A.; Yamamoto, Y.; Brard, L.; Marks, T. J. *J. Am. Chem. Soc.* **1995**, *117*, 3276.

(45) Lappert, M. F.; Pearce, R. *J. Chem. Soc., Chem. Commun.* **1973**, 126.

Downloaded by CARLI CONSORTIUM on June 29, 2009
Published on September 30, 2003 on http://pubs.acs.org | doi: 10.1021/om0304210

Downloaded by CARLI CONSORTIUM on June 29, 2009
Published on September 30, 2003 on http://pubs.acs.org | doi: 10.1021/om0304210

release of 1 equiv of $SiMe_4$, in 37% conversion after 1 h and 50% after 3 h, reaching a plateau at 90% after 3 days, where no more starting carbyl complex was detected ($\delta$ −0.71 (d, $^2J_{YH}$ = 2.3, 6H, YC$H_2$), 0.27 (s, 27H, SiC$H_3$)).

**(b) Preparative-Scale Reaction.** $YCl_3$ (338 mg, 1.73 mmol) was slurried in THF (15 mL) and stirred at 80 °C for 1 h. The solvent was removed in vacuo, and the solid residue was suspended in pentane (20 mL). The suspension was cooled to −78 °C, $LiCH_2SiMe_3$ (5.2 mL of a 1.0 M solution in pentane, 5.2 mmol) was added by syringe, and the suspension was stirred at 0 °C for 2 h. The suspension was filtered, and the white solid was extracted with pentane (2 × 10 mL). LiCl was filtered off, and a solution of **1a** (578 mg, 1.42 mmol) in pentane (30 mL) was added at 0 °C. The reaction mixture was warmed to room temperature and stirred for 30 h. The solution was filtered and concentrated in vacuo. The crude product was recrystallized from pentane at −35 °C to give pale yellow crystals of **2a** (0.63 g, 68%), which proved suitable for X-ray diffraction. $^1$H NMR ($C_6D_6$, 200 MHz, 20 °C): $\delta$ 8.35 (d, 2H, $^4J_{HH}$ = 2.0, 4,5-H), 8.01 (d, 2H, $^3J_{HH}$ = 8.3, 1,8-H), 7.50 (dd, 2H, $J_{HH}$ = 2.0 and 8.3, 2,7-H), 3.06 (m, 8H, α-$CH_2$ THF), 1.54 (s, 9H, NCC$H_3$), 1.48 (s, 18H, CC$H_3$(Flu)), 1.14 (m, 8H, $\beta$-$CH_2$ THF), 0.89 (s, 6H, SiC$H_3$), 0.24 (s, 9H, $CH_2$SiC$H_3$), −1.11 (d, $J_{YH}$ = 3.3, 2H, YC$H_2$). $^1$H NMR (toluene-$d_8$, 200 MHz, 20 °C): $\delta$ 8.29 (d, 2H, $^4J_{HH}$ = 1.4, 4,5-H), 7.94 (d, 2H, $^3J_{HH}$ = 8.6, 1,8-H), 7.42 (dd, 2H, $J_{HH}$ = 1.4 and 8.6, 2,7-H), 3.03 (m, 8H, α-$CH_2$, THF) 1.49 (s, 9H, NCC$H_3$), 1.45 (s, 18H, CC$H_3$(Flu)), 1.17 (m, 8H, $\beta$-$CH_2$, THF), 0.84 (s, 6H, SiC$H_3$), 0.16 (s, 9H, $CH_2$SiC$H_3$), −1.27 (d, $J_{YH}$ = 3.1, 2H, YC$H_2$). $^1$H NMR (toluene-$d_8$, 300 MHz, −70 °C, slow exchange): $\delta$ 8.51 (s, 1H, 4-H), 8.35 (s, 1H, 5-H), 8.12 (d, 1H, $^3J_{HH}$ = 7.7, 1-H), 7.96 (d, 1H, $^3J_{HH}$ = 7.7, 2-H), 7.90 (d, 1H, $^3J_{HH}$ = 7.7, 8-H), 7.49 (d, 1H, $^3J_{HH}$ = 7.7, 7-H), 3.45 (br s, 2H, α-$CH_2$ THF), 3.19 (br s, 2H, α-$CH_2$ THF), 1.70 (s, 9H, NCC$H_3$), 1.57 (s, 18H, CC$H_3$(Flu)), 1.07 (br s, 4H, $\beta$-$CH_2$ THF), 0.99 (s, 3H, SiC$H_3$), 0.78 (s, 3H, SiC$H_3$), 0.44 (s, 9H, $CH_2$SiC$H_3$), −0.59 (d, $J_{YH}$ = 7.0, 1H, YC$H$H), −1.07 (d, $J_{YH}$ = 7.0, 1H, YCH$H$). $^{13}$C{$^1$H} NMR (benzene-$d_6$, 75 MHz, 20 °C): $\delta$ 141.9, 140.1, 130.9, 124.6, 118.5, 117.4, 82.9 (C-9), 70.3 (α-THF), 55.1 (NC$CH_3$), 37.1 (NC$CH_3$), 35.9 (Flu-C$CH_3$), 33.0 (Flu-CC$H_3$), 30.6 (d, $^1J_{Y-C}$ = 45.2, Y$CH_2$), 25.8 ($\beta$-THF), 6.8 (Si$CH_3$), 5.2 ($CH_2$SiC$H_3$). Anal. Calcd for $C_{39}H_{66}NO_2Si_2Y$: C, 64.52; H, 9.16; N, 1.92. Found: C, 63.86; H, 9.32; N, 2.21.

**NMR-Scale Reaction of $Y(CH_2SiMe_3)_3(THF)_2$ and (3,6-$^t$Bu$_2$C$_{13}$H$_7$)SiPh$_2$NH$^t$Bu (1b). Generation of [(3,6-$^t$Bu$_2$C$_{13}$H$_6$)SiPh$_2$N$^t$Bu]Y(CH$_2$SiMe$_3$)(THF)$_x$ (2b).** An NMR tube was charged with $Y(CH_2SiMe_3)_3(THF)_2$ (39 mg, 0.079 mmol) and **1b** (42 mg, 0.079 mmol). Benzene-$d_6$ (ca. 0.6 mL) was condensed in at −196 °C, and the tube was warmed to 50 °C. The progress of the reaction was monitored periodically by $^1$H NMR spectroscopy. After 48 h at 50 °C, formation of **2b** in 25% conversion vs **1b** (>98% selectivity), but with total exhaustion of the initial yttrium carbyl, was observed. Prolonged heating resulted in progressive decomposition of **2b** to form unidentified, insoluble products. $^1$H NMR (benzene-$d_6$, 200 MHz, 20 °C), selected signals for **2b**: $\delta$ 8.40 (d, 2H, $^4J_{HH}$ = 1.1, 4,5 −H), 8.05−7.96 (m, 4H, 1,2,7,8-H), 7.6−7.1 (m, Si$Ph_2$, overlapped with Si$Ph_2$ protons in **1b**), 3.42 (m, 8H, α-$CH_2$, THF) 1.78 (s, 9H, NCC$H_3$), 1.49 (s, 18H, CC$H_3$(Flu)), 1.38 (m, 8H, $\beta$-$CH_2$, THF), 0.32 (s, 9H, $CH_2$SiC$H_3$), −0.82 (d, $J_{YH}$ = 3.3, 2H, YC$H_2$).

**Reaction of [(3,6-$^t$Bu$_2$C$_{13}$H$_6$)SiMe$_2$N$^t$Bu]Y(CH$_2$SiMe$_3$)(THF)$_2$ (2a) with $H_2$ or $PhSiH_3$. Preparation of "{[(3,6-$^t$Bu$_2$C$_{13}$H$_6$)SiMe$_2$N$^t$Bu]Y(H)(THF)}$_2$" (3). Method A.** To a solution of **2a** (100 mg, 0.137 mmol) in benzene (5 mL) was added $PhSiH_3$ (85 mL, 0.688 mmol) at 20 °C. The mixture was stirred at this temperature for 1 h, over which period a yellow precipitate formed. The latter was filtered, washed with benzene (ca. 2 mL), and dried in vacuo to give a pale yellow microcrystalline product insoluble in THF and hydrocarbons (**3**; 70 mg, 90%).

**Method B.** A solution of **2a** (125 mg, 0.172 mmol) in benzene (5 mL) was exposed to a dihydrogen atmosphere (1 bar) at 20 °C for 12 h to yield after similar workup a pale yellow insoluble product with similar characteristics (30 mg, 31%). Anal. Calcd for $C_{62}H_{96}N_2O_2Si_2Y_2$: C, 65.59; H, 8.52; N, 2.47. Found: C, 63.85; H, 8.45; N, 2.49.[46]

**[(3,6-$^t$Bu$_2$C$_{13}$H$_6$)SiMe$_2$N$^t$Bu]Li$_2$(THF)$_3$ (4).** To a solution of **1a** (120 mg, 0.294 mmol) in THF (20 mL) at −40 °C was added with stirring 2 equiv of $^n$BuLi (0.37 mL of a 1.6 M solution in hexane, 0.588 mmol). The reaction mixture was warmed to room temperature and stirred for 8 h. Volatiles were removed under vacuum to yield [(3,6-$^t$Bu$_2$C$_{13}$H$_6$)SiMe$_2$-N$^t$Bu]Li$_2$ as a bright orange powder (172 mg, 92%). Crystals of **4** suitable for X-ray diffraction were grown from a THF/pentane solution at −35 °C.

**[(3,6-$^t$Bu$_2$C$_{13}$H$_6$)SiMe$_2$NH$^t$Bu]Li(DME) (5).** To a solution of **1a** (100 mg, 0.245 mmol) in DME (20 mL) at −40 °C was added with stirring 1 equiv of $^n$BuLi (0.15 mL of a 1.6 M solution in hexane, 0.245 mmol). The reaction mixture was warmed to room temperature and stirred for 8 h. Volatiles were removed under vacuum to give in quantitative yield [(3,6-$^t$Bu$_2$C$_{13}$H$_6$)SiMe$_2$NH$^t$Bu]Li as an orange powder. Crystals of **5** suitable for X-ray diffraction were grown from a DME/pentane solution at −35 °C.

**Salt Elimination Reaction between [(3,6-$^t$Bu$_2$C$_{13}$H$_6$)-SiMe$_2$N$^t$Bu]Li$_2$ (4) and YCl$_3$(THF)$_{3.5}$ (1:1). Preparation of [{(3,6-$^t$Bu$_2$C$_{13}$H$_6$)SiMe$_2$N$^t$Bu}$_2$Y]$^-$[Li(THF)$_4$]$^+$ (6).** To a solution of **1a** (108 mg, 0.265 mmol) in $Et_2O$ (20 mL) at −10 °C was added with stirring 2 equiv of $^n$BuLi (0.33 mL of a 1.6 M solution in hexane, 0.530 mmol). The reaction mixture was warmed to room temperature and stirred for 8 h. To the resulting orange solution cooled to −20 °C was added a suspension of $YCl_3(THF)_{3.5}$ (previously prepared from 52 mg (0.265 mmol) of $YCl_3$) in $Et_2O$ (30 mL). The mixture was stirred and warmed to room temperature; it turned yellow after 30−40 min. The yellow solution was decanted from the precipitate, volatiles were removed in vacuo, and the resulting residue was washed with pentane (2 × 20 mL) to give a yellow powder (101 mg). $^1$H NMR indicated the presence of two species in a 1.4:1 ratio; $^1$H NMR(THF-$d_8$, 200 MHz, 20 °C): major product, $\delta$ 7.89 (d, 2H, $^4J_{HH}$ = 2.1, 4,5-H), 7.69 (d, 2H, $^3J_{HH}$ = 8.6, 1,8-H), 6.90 (dd, 2H, $J_{HH}$ = 2.1, 8.6, 2,7-H), 1.36 (s, 18H, CC$H_3$(Flu)), 1.20 (s, 9H, NCC$H_3$), 0.38 (s, 6H, SiC$H_3$); minor product, $\delta$ 7.83 (m, 2H, $^4J_{HH}$ = 2.1, 4,5-H), 7.54 (d, 2H, $^3J_{HH}$ = 8.6, 1,8-H), 6.84 (dd, 2H, $J_{HH}$ = 2.1, 8.6, 2,7-H), 1.35 (s, 18H, CC$H_3$(Flu)), 1.11 (s, 9H, NCC$H_3$), 0.40 (s, 6H, SiC$H_3$). The crude product was recrystallized from $Et_2O$/THF/pentane (ca. 0.5:1:3) to give yellow crystals of **6** (88 mg, 25%). $^1$H NMR (THF-$d_8$, 300 MHz, 20 °C): $\delta$ 7.94 (d, 2H, $^4J_{HH}$ = 1.8, 4,5-H), 7.72 (d, 2H, $^3J_{HH}$ = 8.3, 1,8-H), 7.13 (dd, 2H, $J_{HH}$ = 1.8, 8.3, 2,7-H), 1.43 (s, 9H, NCC$H_3$), 1.36 (s, 18H, CC$H_3$(Flu)), 0.27 (s, 6H, SiC$H_3$). $^{13}$C-{$^1$H} NMR (THF-$d_8$, 75 MHz, 20 °C): $\delta$ 144.6, 137.8, 133.7, 121.1 (C-1,8), 120.0 (C-2,7), 115.5 (C-4,5), 79.0 (C-9), 54.7 (NC$CH_3$), 36.9 (NC$CH_3$), 35.4 (Flu-C$CH_3$), 33.2 (Flu-CC$H_3$), 6.2 (Si$CH_3$). Anal. Calcd for $C_{70}H_{110}N_2O_4LiSi_2Y$: C, 69.86; H, 9.21; N, 2.33. Found: C, 69.05; H, 8.96; N, 2.38.

**Salt Elimination Reaction between [(3,6-$^t$Bu$_2$C$_{13}$H$_6$)-SiMe$_2$N$^t$Bu]Li$_2$ (4) and LaCl$_3$(THF)$_{1.5}$ (1:1). Preparation of [{(3,6-$^t$Bu$_2$C$_{13}$H$_6$)SiMe$_2$N$^t$Bu}$_2$La]$^-$[Li(THF)$_4$]$^+$ (7).** The same procedure as that described above was carried out from $LaCl_3(THF)_{1.5}$ (previously prepared from 186 mg, 0.758 mmol of $LaCl_3$) and **1a** (310 mg, 0.760 mmol) to give a yellow microcrystalline solid (440 mg). The $^1$H NMR spectrum of this crude product showed that it contains two species in a 1.2:1 ratio. $^1$H NMR (THF-$d_8$, 200 MHz, 20 °C): major product, $\delta$ 7.93 (d, 2H, $^4J_{HH}$ = 2.0, 4,5-H), 7.73 (dd, 2H, $J_{HH}$ = 0.5, 8.6,

(46) Low carbon values were repetitively obtained. We ascribe this problem to the presence of silicon, which is known to form noncombustible SiC. Similar difficulty in obtaining satisfactory elemental analyses for hydrido constrained-geometry or silicon-containing complexes of group 3 metals has been encountered by other workers; see refs 5b,c and: Mitchell, P.; Hajela, S.; Brookhart, S. K.; Hardcastle, K. I.; Henling, L. M.; Bercaw, J. E. *J. Am. Chem. Soc.* **1996**, *118*, 1045.

Downloaded by CARLI CONSORTIUM on June 29, 2009
Published on September 30, 2003 on http://pubs.acs.org | doi: 10.1021/om0304210

1,8-H), 6.94 (dd, 2H, $J_{HH}$ = 2.1, 8.6, 2,7-H), 1.41 (s, 18H, CC$H_3$-(Flu)), 1.24 (s, 9H, NCC$H_3$), 0.44 (s, 6H, SiC$H_3$); minor product, $\delta$ 7.83 (m, 2H, $^4J_{HH}$ = 2.1, 4,5-H), 7.54 (d, 2H, $J_{HH}$ = 8.6, 1,8-H), 6.84 (dd, 2H, $J_{HH}$ = 2.1, 8.6, 2,7-H), 1.35 (s, 18H, CC$H_3$-(Flu)), 1.16 (s, 9H, NCC$H_3$), 0.42 (s, 6H, SiC$H_3$). Recrystallization of the crude product from a 1:4 THF/pentane mixture gave pale orange crystals of **7** (380 mg, 81%). $^1$H NMR (THF-$d_8$, 300 MHz, 20 °C): $\delta$ 7.82 (d, 2H, $^4J_{HH}$ = 1.8, 4,5-H), 7.53 (d, 2H, $^3J_{HH}$ = 8.2, 1,8-H), 6.84 (dd, 2H, $J_{HH}$ = 1.8, 8.2, 2,7-H), 1.35 (s, 18H, CC$H_3$(Flu)), 1.12 (s, 18H, NCC$H_3$), 0.40 (s, 6H, SiC$H_3$). $^{13}$C{$^1$H} NMR (THF-$d_8$, 75 MHz, 20 °C): $\delta$ 144.4, 131.4, 127.7, 119.5 (C-1,8), 118.5 (C-2,7), 114.9 (C-4,5), 84.4 (C-9), 50.7 (N*C*CH$_3$), 35.5 (Flu-*C*CH$_3$), 35.4 (NC*C*H$_3$), 34.1 (Flu-C*C*H$_3$), 6.9 (Si*C*H$_3$). Anal. Calcd for $C_{70}H_{110}N_2O_4LiSi_2La$: C, 67.49; H, 8.90; N, 2.25. Found: C, 67.31; H, 8.37; N, 2.40.

**Salt Elimination Reaction between [(3,6-$^t$Bu$_2$C$_{13}$H$_6$)-SiMe$_2$N$^t$Bu]Li$_2$ (4) and LaCl$_3$(THF)$_{1.5}$ (1:1). Synthesis of [$\eta^3$:$\eta^1$-{(3,6-$^t$Bu$_2$-C$_{13}$H$_6$)SiMe$_2$N$^t$Bu}$_2$La]$^-$[Li(Et$_2$O)$_2$]$^+$ (8).** To a solution of **1a** (340 mg, 0.834 mmol) in Et$_2$O (30 mL) at −10 °C was added with stirring 2 equiv of $^n$BuLi (1.0 mL of a 1.6 M solution in hexane, 1.66 mmol). The reaction mixture was warmed to ambient temperature and stirred for 8 h. To the resulting orange solution cooled to −35 °C in the glovebox was added LaCl$_3$(THF)$_{1.5}$ (295 mg, 0.834 mmol). The mixture was stirred and warmed to room temperature; it turned orange-yellow after 20 min. After 12 h, the yellow solution was decanted from the precipitate and concentrated in vacuo and hexane (ca. 2 mL) was added. Orange-yellow crystals of **8**, which proved suitable for X-ray diffraction, were recovered after 10 h (300 mg, 33%). $^1$H NMR (THF-$d_8$, 200 MHz, 60 °C): $\delta$ 7.79 (d, 4H, $^4J_{HH}$ = 2.0, 4,5-H), 7.25 (d, 4H, $J_{HH}$ = 8.4, 1,8-H), 7.00 (dd, 4H, $J_{HH}$ = 2.0, 8.4, 2,7-H), 3.36 (q, 8H, C$H_2$OCH$_3$), 1.51 (s, 18H, NCC$H_3$), 1.36 (s, 36H, CC$H_3$(Flu)), 1.08 (t, 12H, CH$_2$OC$H_3$), 0.17 (s, 12H, SiC$H_3$). $^{13}$C{$^1$H} NMR (THF-$d_8$, 75 MHz, 60 °C): $\delta$ 144.7, 134.7, 119.5, 114.7 (C-1,8), 130.5 (C-10,13), 117.5 (C-11,12), 81.9 (C-9), 54.9 (N*C*CH$_3$), 35.5 (Flu-*C*CH$_3$), 37.0 (NC*C*H$_3$), 34.7 (Flu-C*C*H$_3$), 7.7 (Si*C*H$_3$). Anal. Calcd for $C_{62}H_{98}N_2O_2Si_2LaLi$: C, 67.36; H, 8.93; N, 2.53. Found: C, 68.23; H, 8.54; N, 2.45.

**Salt Elimination Reaction between [(3,6-$^t$Bu$_2$C$_{13}$H$_6$)-SiMe$_2$N$^t$Bu]Li$_2$ (4) and NdCl$_3$(THF)$_2$ (1:1). Synthesis of [$\eta^3$:$\eta^1$-{(3,6-$^t$Bu$_2$C$_{13}$H$_6$)SiMe$_2$N$^t$Bu}$_2$Nd(THF)]$^-$[Li-(THF)$_4$]$^+$ (9) and [$\eta^5$:$\eta^1$-{(3,6-$^t$Bu$_2$C$_{13}$H$_6$)SiMe$_2$N$^t$Bu}Nd($\mu$-Cl)(THF)]$_2$ (10).** The same procedure as that described above for the preparation of **6** was carried out from NdCl$_3$(THF)$_2$ (245 mg, 0.623 mmol) and **1a** (253 mg, 0.623 mmol) to yield a yellow microcrystalline solid (390 mg). The $^1$H NMR spectrum of this product displayed very broad resonances and proved uninformative. Crystallization of the crude product from a 1:5:3 THF/toluene/pentane solution gave golden yellow crystals of **9**, which proved suitable for X-ray diffraction (40 mg, 10%). Anal. Calcd for $C_{85}H_{134}LiN_2O_6Si_2Nd$ (**9**·THF·(toluene)): C, 68.64; H, 9.08; N, 1.88. Calcd for $C_{74}H_{118}LiN_2O_5Si_2Nd$ (**9**): C, 67.17; H, 8.99; N, 2.12. Found: C, 67.60; H, 8.74; N, 2.41. In another experiment, the crude product was recrystallized from a 5:1 Et$_2$O/hexane solution to afford green crystals of neutral complex **10**, some of which were also found suitable for X-ray crystallographic studies (150 mg, 38%). Anal. Calcd for $C_{62}H_{94}Cl_2N_2O_2Si_2Nd_2$ (**10**): C, 56.63; H, 7.20; N, 2.13; Cl, 5.39. Found: C, 57.01; H, 7.61; N, 1.82; Cl, 4.73.

**Crystal Structure Determinations of Complexes 2a, 4, 5, and 8−10.** Suitable single crystals of all investigated compounds were mounted onto glass fibers using the "oil-drop" method. All diffraction data were collected at 100−120 K using a NONIUS Kappa CCD diffractometer with graphite-monochromated Mo K$\alpha$ radiation ($\lambda$ = 0.710 73 Å). A combination of $\omega$ and $\varphi$ scans was carried out to obtain at least a unique data set. Crystal structures were solved by means of the Patterson method, and remaining atoms were located from difference Fourier synthesis followed by full-matrix least-squares refinement based on $F^2$ (programs Shelxs-97 and Shelxl-97).[47] Many hydrogen atoms could be found from the difference Fourier map. Carbon-bound hydrogen atoms were placed at calculated positions and forced to ride on the attached carbon atom. The hydrogen atom contributions were calculated but not refined. All non-hydrogen atoms were refined with anisotropic displacement parameters. The locations of the largest peaks in the final difference Fourier map calculation and the magnitude of the residual electron densities were of no chemical significance (note that in **5** two peaks were observed near the La atom with an electronic density of ca. 2.5 e Å$^{-3}$; however, the distance being lower than the van der Waals radii, these were not considered). The cell of **4** was found to contain one molecule of crystallization of toluene and that of **9** one toluene molecule and one THF molecule. Crystal data and details of the data collection and structure refinement are given in Table 1. Atomic coordinates, thermal parameters, and complete listings of bond lengths and angles are available as Supporting Information.

**Typical Procedure for Ethylene Polymerization.** Toluene (50 mL) was introduced in a 300 mL glass reactor (TOP-Industrie) equipped with a mechanical stirrer rotating at speeds up to 1500 rpm. Toluene was saturated with ethylene (Air Liquide, N35; 4 atm, kept constant via a back-pressure regulator). At the same time, a mixture of chloroneodymium complex **10** (163 mg; 0.248 mmol) and LiCH(SiMe$_3$)$_2$ (41 mg, 0.248 mmol) in toluene (10 mL) was stirred for 1 h at 20 °C. The resulting pale green solution was then transferred via syringe into the reactor with stirring. The ethylene flow rate was monitored using a mass flowmeter (Aalborg, GFM17) connected to a totalizing controller (KEP) which acts as a flow rate integrator. The reaction was quenched by addition of 3 mL of a 10% HCl methanol solution to the mixture. The resulting precipitate was filtered, washed with methanol, and dried under vacuum.

**Typical Procedure for MMA Polymerization.** In a Schlenk tube containing a magnetic stir bar and solid recrystallized complex **7** (20 mg, 0.016 mmol) (in 10−15 mL of toluene for reactions carried out in solution), methyl methacrylate (ACROS, previously dried from CaH$_2$; 1.0 mL, 9.3 mmol) was added by syringe and vigorous stirring at the appropriate temperature was immediately started. After 12 h, the Schlenk tube was opened to air and acetone (30 mL) was added to quench the reaction and dissolve the polymer formed. The polymer was precipitated by adding methanol (ca. 200 mL), filtered, washed twice with methanol (30 mL), and dried in vacuo. The number-average molecular weight $M_n$ and the weight-average molecular weight $M_w$ were determined by GPC in THF using universal calibration relative to polystyrene standards. The polymer microstructure was determined by $^1$H NMR in CDCl$_3$.

**Acknowledgment.** We gratefully thank TotalFinaElf for supporting this research (postdoctoral fellowship to E.K.). We are most grateful to Mr. V. Bellia (AtoFina) for technical support and to Mr. S. Foley and Prof. R. F. Jordan (University of Chicago) for GPC analysis of the PE sample.

**Supporting Information Available:** Details of structure determinations of complexes **2a**, **4**, **5**, and **8**−**10**, as well as that of free ligand **1a**, including final coordinates, thermal parameters, bond distances, and bond angles. This material is available free of charge via the Internet at http://pubs.acs.org.

OM0304210

(47) (a) Sheldrick, G. M. SHELXS-97, Program for the Determination of Crystal Structures; University of Göttingen, Göttingen, Germany, 1997. (b) Sheldrick, G. M., SHELXL-97, Program for the Refinement of Crystal Structures; University of Göttingen, Göttingen, Germany, 1997.